COLLEGE OF NATURAL AND COMPUTATIONAL SCIENCE

SCHOOL OF EARTH SCIENCE

PETRO-CHEMICAL CHARACTERIZATION OF BASEMENT PLUTONIC ROCKS AND ASSOCIATED VOLCANIC OUTCROPS IN HOMOSHA-KURMUK AREA, WESTERN ETHIOPIA.

A thesis submitted to the School of Earth Sciences at Addis Ababa University in partial completion of the requirements for the degree of Masters in Petrology

By: ASEDIK ALESA

I.D.NO. GSR/3191/14

Advisor: SOFIA ABDULKADIR (Ph.D.)

May 2023, Addis Ababa, Ethiopia

ADDIS ABABA UNIVERSTY

COLLEGE OF NATURAL AND COMPUTATIONAL SCIENCE

SCHOOL OF EARTH SCIENCE

PETRO-CHEMICAL CHARACTERIZATION OF BASEMENT PLUTONIC ROCKS AND ASSOCIATED VOLCANIC OUTCROPS IN HOMOSHA-KURMUK AREA, WESTERN ETHIOPIA.

By: ASEDIK ALESA

ID.NO. GSR/3191/14

May 2023 Addis Ababa, Ethiopia

Declaration of originality

I hereby declare that I completed the "Petro-Chemical Characterization of Basement Plutonic Rocks and Associated Volcanic Outcrops in Homosha-Kurmuk Area, Western Ethiopia" dissertation in the academic year 2022-2023 under the guidance of Dr. Sofia Abdulkadir at the School of Earth Science, Addis Ababa University, Addis Ababa. I additionally certify that this work has not been submitted to any other university or institution for the purpose of receiving a degree or diploma.

Place: Addis Ababa

Date: 2023

(BY ASEDIK ALESA)

ADDIS ABABA UNIVERSTY

COLLEGE OF NATURAL AND COMPUTATIONAL SCIENCE

SCHOOL OF EARTH SCIENCE

PETRO-CHEMICAL CHARACTERIZATION OF BASEMENT PLUTONIC ROCKS AND ASSOCIATED VOLCANIC OUTCROPS IN HOMOSHA-KURMUK AREA, WESTERN ETHIOPIA.

By: ASEDIK ALESA

I.D.NO. GSR/3191/14

A thesis presented to the Addis Ababa University School of Earth Sciences in partial completion of the criteria for the degree of Masters in Petrology.

Approved by board of examiners:

Prof. Worash Getaneh	__________	___________
Chairman	Signature	Date
Dr. Sofia Abdulkadir	____________	_____________
Advisor	Signature	Date
Prof. Gezahegn Yirgu	____________	______________
Examiner	Signature	Date
Prof. Dereje Ayalew	_____________	_______________
Examiner	Signature	Date

Acknowledgments

I would want to offer my sincere gratitude and appreciation to all who helped me successfully complete this research effort. Hence,

I want to express my gratitude to Assosa University for supporting my pursuit of an MSc in petrology. Second, I want to thank Addis Ababa University and the School of Earth Science for accepting me and providing me with the necessary resources to finish my studies. My advisor, Dr. Sofia Abdulkadir, has my deepest gratitude and appreciation for all of her suggestions, follow-ups, and invaluable assistance with my thesis. I want to thank my friend Mr. Mujahed Ibrahim for all of his assistance both before and after my fieldwork. My sincere gratitude also extends to Mr. Ejara, the lab manager of the Institute of Geological Survey of Ethiopia, for enabling payment-free sample preparation. Additionally, I want to thank the administrators of Kurmuk and Homosha Woreda for providing me with all the assistance I needed while working in the field. Last but not least, I want to express my gratitude to the communities living in the study area for all the wonderful memories.

Abstract

The primary objective of this study was to characterize the petrography and geochemistry of the rocks in the study area with the goal to determine the classification of the lithological units that were discovered there. Field investigation, petrographic study, and a complete silicate geochemical analysis were done for this aim. According to the petrographic findings, the primary components of the rock units in the research region are quartz, plagioclase, k-feldspar, olivine, pyroxenes, biotite, hornblende, and opaque minerals. According to the TAS classification, the geochemical findings identified the rock units in the research region as granite, basalt, rhyolite, and diorite. Additionally, it placed the mafic/basaltic samples in the tholeiitic series on AFM and the felsic samples in the calc-alkaline series. The rock units in the studied area are thought to have formed as a result of fractional crystallization combined with crustal contamination, according to the Harker variation diagram of the major oxides versus SiO2. This fact is demonstrated by the fact that while the concentration of the major oxides like Na2O and K2O displays an increasing pattern with the increasing SiO2 concentration, the concentration of the major oxides like TiO_2, Al_2O_3, MgO, CaO, P_2O_5 and FeOt decreases with the increasing concentration of SiO2. The granites are determined **to** be of post-tectonic origion at continental arcs while the basalts are determined to be of subduction zones.

Key words: Dul-Undu, Gule, Homosha-Kurmuk, volcanic outcrops

Table of contents

Contents

Acknowledgments i
Abstract ii
Table of contents iii
List of figures vi
List of acronyms viii
CHAPTER ONE 1
Introduction 1
1.1 General background 1
1.2 Description of 'the study area' 3
1.2.1 Location 3
1.2.2 Physiography and drainage of the study area 4
1.2.3 Vegetation and climate 5
1.2.4 Population and land use 6
1.3 Problem statement 6
1.4 Significance of the study 7
1.5 Objectives 7
1.5.1 General Objective 7
1.5.2 Specific Objectives 7
1.6 Limitations 7
1.7 Organization of the Thesis 8
CHAPTER TWO 9
Literature Review 9
2.1 Previous works 9
2.2 Regional Geology 9
2.2.1 Birbir Domain 13
2.2.2 Geba Domain 13
2.2.3 Baro Domain 13

2.2.4 Didesa domain 13
2.2.5 Kemashi domain 14
2.2.6 Dengi domain 14
2.2.7 Sirkole domain 15
2.2.8 Daka domain 15
a) Gimbi Terrane 16
b) Nejo Terrane 18
c) Assosa Terrane 18
CHAPTER THREE 21
Materials and methodology 21
CHAPTER FOUR 23
LOCAL GEOLOGY OF ‘THE STUDY AREA’ 23
4.1 Massive Basalts 23
4.2 Quartz infill 24
4.3 Jointed basalts 25
4.4 Rhyolites 27
4.5 granitic rocks 27
4.6 Diorite 28
4.6 Quartz vein 29
CHAPTER FIVE 31
PETROGRAPHY OF ‘THE STUDYAREA’ 31
CHAPER SIX 41
RESULTS AND INTERPRETATIONS 41
6.1 Petrography 41
6.1.1 The QAP plot of granites 42
6.2 Geochemistry 43
6.2.1 Classification of rocks in the research area Based on silica content 44
6.2.2 The TAS classification of Rocks of the research area 44
6.3 AFM classification 50
CHAPTER SEVEN 51

DISCUSSIONS AND SUMMARY 51
7.1 Introduction 51
7.2 Geology of the study area........ 51
7.3 Petrography 52
7.4 Geochemistry and fractional crystallization........ 53
7.5 Geotectonic settings 55
CHAPTER EIGHT 59
CONCLUSIONS AND RECOMMENDATIONS 59
8.1 Conclusions 59
Recommendations 60
References........ 61
Appendixes 79
Appendix-1 Field description of the representative rock samples 79
Appendix-2 modal percentage of the minerals seen under petrographic microscope in the representative samples........ 80
Appendix-3: definition of terms........ 80

List of figures

FIGURE 1: THE MAP OF ARABIAN-NUBIAN SHIELD (AFTER STERN ET. AL., 1990) 3
FIGURE 2: LOCATION AND ACCESIBLITY OF THE STUDY AREA.. 4
FIGURE 3 PHYSIOGRAPHIC MAP OF 'THE STUDY AREA' 5
FIGURE 4: CLIMATIC DIAGRAM SHOWING AVERAGE ANNUAL TEMPERATURE AND RAINFALL OF HOMOSHA DISTRICT FOR 9 YEARS. (2009-2017). 6
FIGURE 5: THE GEOLOGICAL MAP OF TULUDIMTU BELT IN WESTERN ETHIOPIA 16
FIGURE 6: THE MAP OF DUL'S GEOLOGY AND THE SURROUNDING TERRITORIES (ADAPTED FROM WOLLIE SHEKA ET AL., 1990; MERSHA JEMBERE ET AL., 1995 AS IN ZAKARIA HAMIMI ET AL., 2021)... 20
FIGURE 7 THE DIAGRAM SHOWING METHODOLOGY 22
FIGURE 8: MASSIVE BASALTS: A, THE FIELD PHOTOGRAPH AT MOUNTAIN DUL UNDU B&C THE FIELD PHOTOGRAPHY OF VOLCANICS AND CHALKY ROCKS APPEARED AS A VEIN IN VOLCANIC GROUNDMASS AT A ROAD CUT EXPOSURE ON THE FLAT TOPOGRAPHY AROUND THE DUL-UNDU MOUNTAIN. 24
FIGURE 9: QUARTZ INFILL SEEN ON THE AMYGDALOIDAL BASALTS S IN 'THE STUDY AREA' (FROM FIELD PHOTOGRAPH).. 24
FIGURE 10: WHEATHERED BASALTS WITH RHYOLITES: A, WHEATHERED BASALT B, THE LAYERED ROCK THAT OVERLYING IT DETERMINED GEOCHEMICALLY AS A RHYOLITE AND JOINTING IN BASALT NEAR BAMADHON VILLAGE OF HOMOSHA WOREDA 26
FIGURE 11: UNWEATHERED BASALTS; A, AROUND HOMOSHA, B, NEAR UNDU 26
FIGURE 12: RHYOLITIC EXPOSURES IN 'THE STUDY AREA'; A, THE SMOOTH WHITISH ROCK AT THE FOOT AND B, AT THE TOP MOST OF UNDU MOUNTAIN. 27
FIGURE 13: GRANITIC EXPOSURES; A, COARSE GRAINED GRANITE, B, FINE TO MEDIUM GRAINED GRANITE, C, SMALL QUARTZ VEINS ON GRANITE, D, CIRCULAR STRUCTURES, E, GRANITIC INTERGROWTH, AND F MEDIUM TO COARSE GRAINEDGRANITIC OUTCROP AWAY FROM UNDU MOUNTAIN. 28
FIGURE 14: A) THE 'CONTACT' BETWEEN THE GRANITE AND THE QUARTS AND BIOTITE DOMINATED DARK GREENISH ROCK (DIORITE), B) THE PINKISH COLORED GRANITE. 29
FIGURE 15: QUARTZ VEIN OBSERVED IN THE AREA OF STUDY.. 29
FIGURE 16: THE GEOLOGIC MAP OF THE STUDY AREA 30
FIGURE 17: SAMPLE D2S1; A, HAND SPECIMEN, B&C SHOWS THE GENERAL XPL AND PPL VIEWS OF THE THIN SECTION, WHILE D&E SHOWS THE XPL AND PPL OF THE OBSERVED MINERALS RESPECTIVELY. 32
FIGURE 18: HAND SPECIMEN AND MICRO-PHOTOGRAPHY OF SAMPLE D1S1; A, HAND SPECIMEN; B, XPL VIEW AND C, THE PPL VIEW OF THE SAMPLE THIN SECTION D1S2 COLLECTED FROM DUL UNDU MOUNTAIN.. 33
FIGURE 19: HAND SPECIMEN AND MICRO-PHOTOGRAPHY OF SAMPLE D3S1; A, HAND SPECIMEN, B&D XPL, C&E, PPL.. 34

FIGURE 20: HAND SPECIMEN AND MICROPHOTOGRAPHY OF SAMPLE D2S2; A, HAND SPECIMEN;B&D SHOWS DIFFERENT VIEWS OF D2S2 IN XPL WHILE C&E& SHOWS PPL VIEWS OF THE SAMPLE. 36
FIGURE 21: HAND SPECIMEN AND MICRO-PHOTOGRAPHY OF SAMPLES D3S2 AND D2S5; A&B, HAND SPECIMENS; C&E, XPL AND D&F, PPL VIEWS OF SAMPLES D3S2& D2S5 RESPECTIVELY...... 37
FIGURE 22: HAND SPECIMEN AND MICRO-PHOTOGRAPHY OF SAMPLE D3S7&D4S1G; A&B HAND SPECIMENS; C&E XPL AND D&F PPL VIEWS OF THIN SECTION OF D3S7& D4S1G RESPECTIVELY. 39
FIGURE 23: HAND SPECIMEN AND MICRO-PHOTOGRAPHY OF SAMPLE D4S1; A, HAND SPECIMEN; B THE XPL WHILE C IS THE PPL VIEWS OF THE MINERALS SEEN IN SAMPLE D4S1 THIN SECTION 40
FIGURE 24: THE QAP CLASSIFICATION OF GRANITES........ 42
FIGURE 25: TAS CLASSIFICATION OF THE PLUTONIC SAMPLES FROM THE STUDY AREA; MIDDLEMOST (1994)........ 45
FIGURE 26: TAS CLASSIFICATION OF THE META-VOLCANIC ROCK SAMPLES FROM THE STUDY AREA AFTER LE BAS ET AL. (1986) 46
FIGURE 27: PLOTS OF MAJOR OXIDE VS SILICA CONTENT OF PLUTONIC 'SAMPLES' FROM THE RESEARCH AREA, AND SOUTH OF THE STUDY AREA FROM THE WORK OF NATNAEL WONDERA (2018); A TiO_2 VS SiO_2, B Al_2O_3 VS SiO_2, C MGO VS SiO_2, D CAO VS SiO_2, E Na_2O VS SiO_2, F K_2O VS SiO_2, G P_2O_5 VS SiO_2, H FEO(T) VS SiO_2........ 48
FIGURE 28: MAJOR OXIDES VS SILICA PLOT OF VOLCANIC SAMPLES 49
FIGURE 29: AFM PLOT OF REPRESENTATIVE ROCK SAMPLES OF THE 'RESEARCH AREA' AFTER IRVIN AND BARGAR (1971) 50
FIGURE 30: PLOTS OF MAJOR OXIDES VS SILICA OF PLUTONIC SAMPLES; A, TiO_2 VS SiO_2; B Al_2O_3 VS SiO_2; C, MGO VS SiO_2; D, CAO VS SiO_2, E, Na_2O VS SiO_2; F, K_2O VS SiO_2; G, P_2O_5 VS SiO_2, AND H, FEOT VS SiO_2 54
FIGURE 31: MAJOR OXIDES VS SiO_2 PLOT OF VOLCANIC SAMPLES; A, TiO_2 VS SiO_2; B Al_2O_3 VS SiO_2; C, MGO VS SiO_2; D, CAO VS SiO_2, E, Na_2O VS SiO_2; F, K_2O VS SiO_2; G, P_2O_5 VS SiO_2, AND H, FEOT VS SiO_2 55
FIGURE 32: THE SYLVESTER DIAGRAM OF GRANITIC ROCKS AFTER SYLVESTER (1989)........ 56
FIGURE 33: THE R1-R2 DIAGRAM OF GRANITIC ROCKS AFTER BATCHELOR AND BOWDEN (1985). 57
FIGURE 34: THE 10MNO-TIO2-10P2O5 DIAGRAM OF BASALTOIDS AFTER MULLEN (1983)........ 58

List of acronyms

- **AAS**: Atomic Absorption spectrometry
- **AFM:** lumina Iron Magnesium Diagram
- **ANS:** Araban Nubian Shield
- **Bt:** biotite
- **cpx** clinopyroxene
- **D2** 2nd defoemation
- **D3** 3rd deformation
- **E** Easting
- **EAO** East African Orogene
- **et al**. and others
- **fld** feldspar
- **GPS** Global Positioning System
- **GRMs** geochemical reference materials
- **hbl** hornblende
- **HF** Hydrogen Fluoride
- **Kbar** kilo bars
- **km** Kilometer
- **LOI** Loss On Ignition
- **m.a.s.l** Meters Above Sea Level
- **M1** First Stage Metamorphism
- **M2** 2nd Stage Metamorphism
- **Ma** Million years
- **MB** Mozambique Belt
- **N** Northings
- **N-E** north east
- **NW** North West
- **olv** olivne
- **opq** opaque
- **plg** plagioclase
- **PPL** Plane Polarized Light
- **PT** pressure/temperature
- **pyx** pyroxene
- **qtz** quartz
- **SES** Southern Ethiopian Shield
- **SSZ** Sirkole Shear Zone
- **TAS** Total Alkali Versus Silica
- **TDBB** Tulu-Dimtu Baruda Belt
- **WES** Western Ethiopian Shield
- **Wt%** weight percentage
- **XPL** Cross Polarized Light
- **XRF** X-Ray Flourescence

CHAPTER ONE

Introduction

1.1 General background

The Arabian-Nubian Shield (ANS), also called the Neoproterozoic Pan African Orogenic Belt, dominates the underlying geology of northeastern Africa and southwestern Arabia. Kennedy (1964) gave the Pan-African thermo-tectonic event its original name and assigned it an age range of 550–450 Ma, but the term has now been expanded to cover all Neoproterozoic orogenesis in Africa from around 850–500 Ma (Kroner, 1984). It can be compared to "the East African Orogen" (EAO) of Stern (1993, 1994), a term used to describe the assembly of Gondwana through the fusion of Gondwana's East and West (McWilliams, 1981), and is thought to represent a multi-stage accretion of various arc terranes and continental fragments (Shackleton, 1996; Kroner €et al., 1999). "The Mozambique Belt" of high-grade gneisses makes up the majority of the EAO in the southern part of East Africa, which includes Madagascar, Mozambique, Malawi, Tanzania, and Kenya (Holmes, 1951). The Pan-African Orogen, also known as the ANS or the Pan-African Orogen, is a more comprehensive term for the volcano-sedimentary, rocks that make up the majority of the EAO in NE Africa and Arabia. There is no clear connection between these two EAO components. In accordance with 'early Rb/Sr whole rock and U/Pb zircon dates', "the Mozambique Belt" (MB) has been assigned an age between 850 and 1100 Ma (Caen-Vachette, 1977, 1979; Andreoli, 1981; Costa et al., 1992; Pinna et al., 1993) and it was initially thought that it was older than the Pan-African Orogen and represented the ANS's basement (Kazmin, 1975). Therefore, in NE Africa, moderate- to high-grade gneisses were believed to reflect the Pan-African Belt's underlying Mozambique Belt, while relatively young ages found in East Africa's Mozambique Belt were linked to Pan-African rework (Cahen et al., 1984). The substitute and presently more prevalent theory postulates that the ANS and MB evolved while maintaining structural and metamorphic consistency during 'the Pan African Orogeny', with the difference in grade reflecting a collision that was more intense in the south than the north (de Wit and Chewaka, 1981; Almond, 1983; Shackleton, 1986; Stern and Dawoud (1991), Berhe (1990), Key et al. (1989). Abraham (1989), Gichile (1992), Tadesse and Tesfeye

(1999), among others, claim that the basement geology of the southwest corner of Ethiopia and southeastern Sudan is composed of a series of low-grade volcano-sedimentary belts that are dispersed with higher-grade gneiss terranes that, in some areas, approach granulite facies grade. Ophiolitic-rich linear zones are typically found in the volcano-sedimentary belts. Examples include the Baragoi and the Sekerr Complexes in northwest Kenya, the Adola-moyale and Tulu-Dimtu Complexes in western and southern Ethiopia, and the Ingessana and Kabus Complexes in southeast Sudan. Precambrian rocks from western Ethiopia's terrain include gneissic terranes, ophiolitic rocks, and volcanic-sedimentary terrain that are comparable to Neoproterozoic rocks from the ANS and rocks from the MB 20, 24-27. High-grade rocks, Dioritic (granodioritic) batholiths, the ophiolite belt, and related transitional volcanic rocks, as well as meta-volcano-sedimentary rocks, are among the lithological elements found in this area (Dereje K., et al., 2021).

As cited in Dereje K, (2017), according to recent studies, the Gore- Gambella area, which includes the ‘domains’ of Birbir, Baro, and Gore (Teklewold Ayalew, 1997), and the Tulu Dimtu belt, which includes five domains, are divided up into the Western Ethiopian basement. ‘Didessa’, ‘Kemashi’, ‘Dengi’, ‘Sirkole’, and ‘Daka’ domains (Allen and Gebremedhin Tadesse, 2003). According to Mengesha Tefera and Berhe (1996), cited in Teklewold Ayalew (1997), the Baro and Geba domains, which contain high-grade rocks including gneisses and migmatites, and the Birbir domain, which contains lower-grade metamorphic rocks, make up the Gore-Gambella's lithotectonic components. Ultramafic, mafic, intermediate, and felsic volcanic bodies have been intruded. The Tuludimtu Belt, which encompasses the Gimbi-Asosa region, is made up of a several different low to moderate-grade meta-sedimentary rocks as well as moderate to high-grade gneisses (Allen & Gebremedhin Tadesse, 2005).

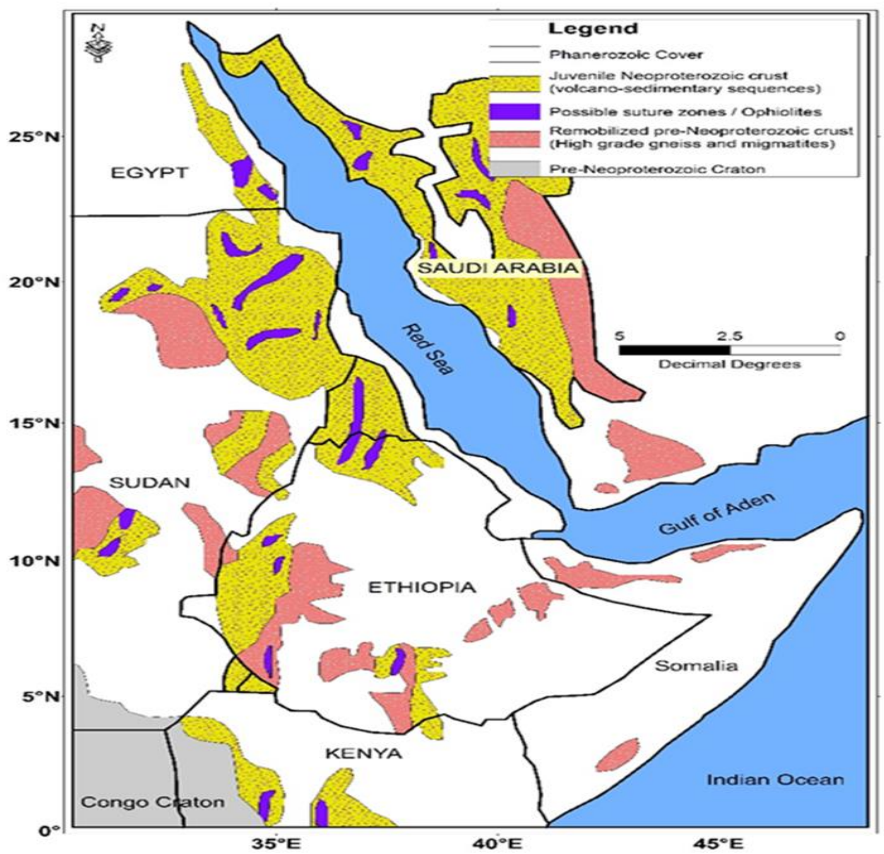

Figure 1: The map of Arabian-Nubian shield (after Stern et. al., 1990)

1.2 Description of 'the study area'

1.2.1 Location

The research area is situated in western Ethiopia's Benishangul Gumuz region, in the Assosa zone. It is situated at latitudes 0665538-0678645 N, longitudes 1135340-1164678 E, and altitude 1312-1611 m a.s.l. The primary asphalt road between Assosa and Kurmuk provides access to the research area, and some of it may be reached on foot or by motorcycle for fieldwork.

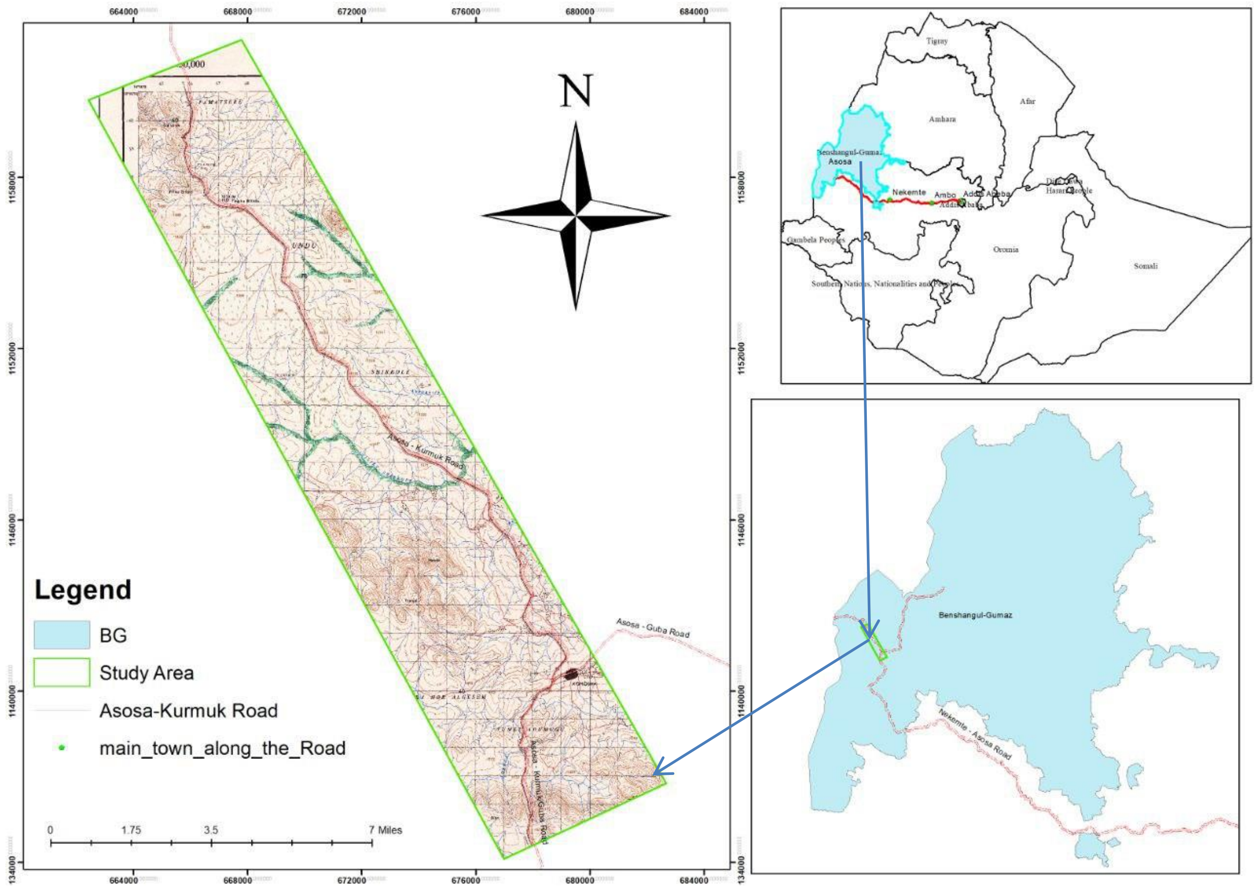

Figure 2: Location and accesiblity of the study area

1.2.2 Physiography and drainage of the study area

The research area has ridges where the rocks are generally exposed and a mostly flat surface. The altitude in the area is between 1312 and 1611 meters. According to 'Allied Gold Corp' (2021), the research region is situated in the western lowlands and has a rough topography with parallel undulating ridges, mountainous ranges, and elevated sections running northeast to southwest. The streams such as Hoha, Tumet, Shirkole, and many others that are tributaries of the Nile are among those that flow throughout the year.

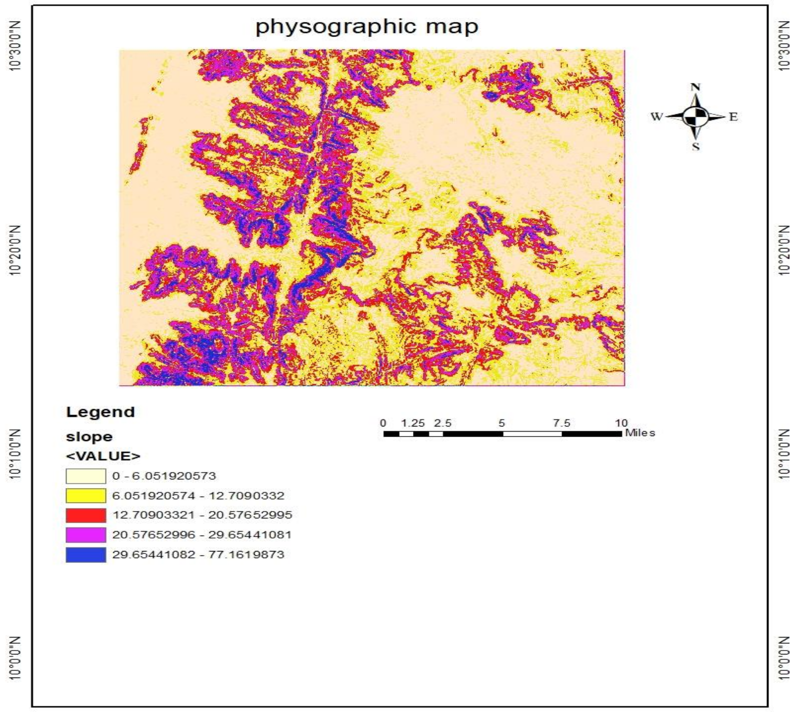

Figure 3 Physiographic map of 'the study area'

1.2.3 Vegetation and climate

Despite the rugged landscape, this area is almost entirely covered by natural vegetation, mainly made up of open grasslands, woody shrub grassland, shrub grassland, dense woodland, and bamboo thicket. The Agency for Metrological Services in Assosa reports that the pattern of distribution of rains is one-modal, extending from the 'end of the month' of April until the beginning of November, with altitudes ranging between 1100 and 1350 meters above sea level. The agency also reports that 'the average annual rainfall' ranges from 588 and 1,549 millimeters. Maximum daily temperatures in the dry season range from 21.4 to 31.5 C, with February to April being the hottest month. Depending on the season and height, the lowest temperature fluctuates from 7.4 to 17.60 degrees.

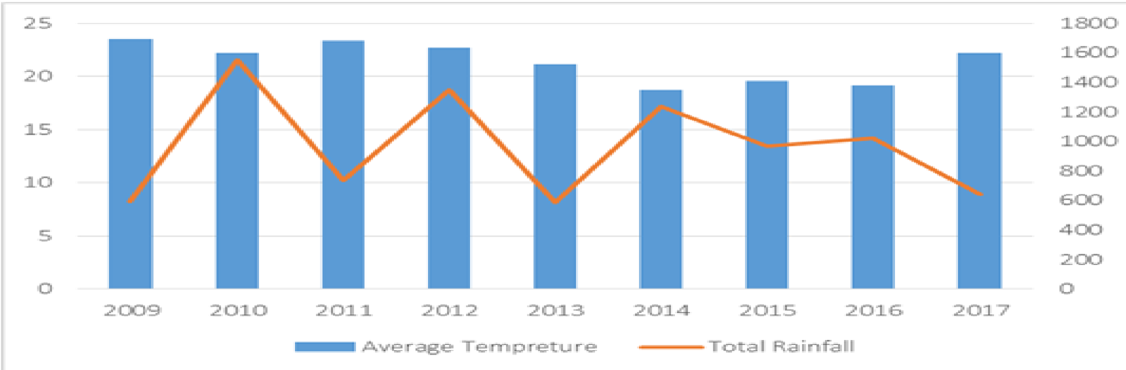

Figure 4: Climatic diagram showing average annual temperature and rainfall of Homosha District for 9 years. (2009-2017).

1.2.4 Population and land use

Both local Benishangul/Berta residents and Sudanese refugees live in the research area. According to information acquired from the Homosah Woreda Agricultural Office, there are 29252 people living in Homosha woreda overall, 14,894 of them are men and 14358 of whom are women. Due to poor weather (high 'temperatures' and high 'humidity'), tsetse fly infestations, and malaria issues, these regions experience minimal population pressure. The locals engage in small-scale sorghum and maize farming as well as conventional gold mining.

1.3 Problem statement

Dereje Kenea (2017) notes that, earlier researchers have worked on regional studies on the geology, geochemistry, and structural geology of the western portion of the Ethiopian basement (Teklewold Ayalew and Johnson, 2002; Tesfaye Kebede and Koeberl, 2002; Allen and Gebremedhin Tadesse, 2003; Tadesse Alemu and Tsegaye Abebe, 2007; Blades, 2013, 2015). However, the area's detailed lithology and petrography have not been well studied. The lithological 'units' of the Homosha-Kurmuk area, which is a component of 'the western Ethiopian basement', have not been 'thoroughly' explored. In order to determine the lithological 'units' in terms of 'geochemistry' and the observed 'mineralogy' in the thin sections obtained for this study, a field investigation, petrographic analysis, and comprehensive silicate analysis of the area are all goals of this work.

1.4 Significance of the study

- As no systematic work has been done in this part of the country, result of this study will provide better understanding of the evolution of the ophiolite belt. It is also be a working guide for a mineral exploration and processing activities for basement hosted mineralization.
- The immediate beneficiaries of this work are the Geological Survey of Ethiopia, government organizations, local and foreign investors working in the mineral resource sector, research organizations and academic institutions of the earth science.
- It will encourage experts to conduct a thorough examination of the region because it is home to valuable natural resources like gold.
- It will make it simpler for businesses to work with or invest in mineral resources. being the principal one, gold

1.5 Objectives

1.5.1 General Objective

The 'main' objective of this study is to characterize the geochemistry and petrography of the lithological units found in Homosha-Kurmuk area

1.5.2 Specific Objectives

- To name and classify the rock units according to petrography and their major oxide concentrations in w%
- To determine the geotectonic setting of rocks found in Homosha-Kurmuk area
- To sketch the geological map of this area
- to construct the variation diagram of the major oxide concentrations of the rocks in 'the study area' that aids in identifying the geochemical processes

1.6 Limitations

The research area is on the border between Ethiopia and Sudan, and a base map of the entire area has not yet 'developed'. Due to this, the study had to focus mostly on Homosha and only a small area of Kurmuk in the vicinity of Famestere village. According to the Ethiopian map agency, even though the map is made, the kurmuk area is not provided to the people because it is situated near borders. The gold firms involved in the study forbid a field geologist from making observations and gathering samples within their licensed territory. Another ‘drawback’ is that grasses conceal a large portion of the exposure, making it challenging to fully and precisely examine the exposures. Another challenge for a field study is the prevalence of desert flies in the study.

1.7 Organization of the Thesis

Eight chapters make up this thesis paper. The history, location, and accessibility of the ‘research’ area are covered in Chapter 1's introduction. This chapter goes into great length about the physiography, population distribution, and vegetation of ‘the study area’ along with the goal, importance, and limitations of this particular study. The second chapter contains a literature review that goes into great detail about the area geological setting and earlier efforts. The materials and methodology used to conduct this research are covered in Chapter 3 of this thesis. Based on observations made and data collected during fieldwork, chapter four discusses the ‘regional geology’ of the area. Chapters five discuss the petrography and chapter six discus the results and interpretations. The explanation of this thesis is in chapter 7, and the conclusion and recommendations are in chapter 8.

CHAPTER TWO

Literature Review

2.1 Previous works

Selamawit Abdissa (2018) has demonstrated that several scholars have investigated the Western Ethiopian Precambrian shield from various angles. As referenced in Tesfaye Kebede et al. (1999), these include Kazmin (1969); De Wit and Aguma; De Wit et al.; and Senbeto Chewaka (1980). The classification of the local Precambrian geology was the main focus of these researches. They have recognized the high-grade gneissic rocks (MB) and the Pan-African low-grade volcano-sedimentary rocks (ANS). In addition, Mengesha Tefera and Seife Michael Berhe (1987) and Moore et al. (1987) did additional research that was cited by Teklewold Ayalew and Johnson (2002). These studies also sought to categorize the local rocks into three known litho-tectonic zones. Studies by Tesfaye Kebede and Koebrel, C. (2001b, 2003); Tesfaye Kebede et al. (1999); Tesfaye Kebede and Koebrel, C. (2001b, 2003); and others have provided more detailed investigations into the region's geology, petrogenesis, geochemistry, tectonic context, and evolution. Allen and Gebremedhin Tadesse (2003, 2005); Johnson et al. (2004); Teklewold Ayalew (1997); Teklewold Ayalew and Johnson (2002); Teklewold Ayalew and Peccerillo (1998); Braathen et al. (2001); Tadesse Yihunie and Fekadu Hailu (2007); and Grebonnikov, A.V. (2014). The dating of granitoids performed by Blades et al. (2015), Teklewold Ayalew et al. (1990), and Tesfaye Kebede et al. (2001) has limited the age of Precambrian rocks in western Ethiopia. As part of the map sheet from Bure project work, Lulu Tsige (2008)'s Ethiopian geological survey examined the petrography of the Precambrian rocks in the Abay (Blue Nile) River canyon. Mengesha Tefera (19991) investigated the Assosa-Kurmuk geology.

2.2 Regional Geology

According to Zakaria Hamimi et al. (2021), ‘the Pan-African belt’ in ‘western Ethiopia’ stretches northward from 6° N for approximately 600 km, with its breadth varying. It is the greatest ‘Precambrian’ exposure in the country and represents the western and ‘wider’ branch of the primarily ‘juvenile terrain’ of the southern ‘Arabian-Nubian Shield’ (ANS). It is ‘wider’ in the north (200–250 km wide) and ‘narrower’ in the south (20–50 km wide). The EAO is frequently used as an ‘example’ of Neoproterozoic Cambrian ‘Wilson’ Cycle ocean basin evolution (Stern, 1994; Worku and Schandelmeier, 1996; Fritz et al., 201), as stated in Shelby Bowden et al. (2020). Zircon U-Pb dating places ‘ANS formation’ in the ‘Neoproterozoic-Early Cambrian’ during ‘Mozambique Ocean closure’, although ‘around 5% of zircons’ in ANS rocks have much older ages, attributed to either ‘mantle’ or ‘detrital’ zircon sourcing by Sr, Nd, Hf, and Pb isotopic ratios (Stern and Kroner, 1993; Stern, 1994; Divi et al., 2001; Stern, 2002; Stern et al., 2010; Johnson et al., 2011; Fritz et al., 2013). A Tibetan-type escape tectonic collision between the ‘ANS’ and East and West ‘Gondwana’ occurred between 750 and 650 Ma, ‘remobilizing’ older MB-related crust and resulting in igneous intrusions throughout the ‘Neoproterozoic’ and Early ‘Cambrian’ (Bonavia and Chorowicz, 1992; Muhongo and Lenior, 1994; Stern, 1994; Abdelsalam and Stern, 1996; Chen, 2001; Muhongo et al. According to several studies (Kebede et al., 1999; Johnson et al., 2004; Abdelsalam et al., 2008; Stern et al., 2012; Blades et al., 2015, 2017), Ethiopia's EAO-related crust is revealed as a succession of constrained basement shields. ‘The Southern Ethiopian Shield’ (SES) and ‘the Western Ethiopian Shield’ (WES), two of the ‘largest’ shields, are situated in ‘southern’ and ‘western’ Ethiopia, respectively (Ayalew and Johnson, 2002; Stern et al., 2012). According to Kebede et al. (1999), Johnson et al. (2004), Abdelsalam et al. (2008), Stern et al. (2012), and Blades et al. (2015), both shields are distinguished by by magmatic intrusion terranes, high-grade gneissic rocks, and accreted volcanic arc. According to several studies (Stern, 1994; Abdelsalam and Stern, 1996; Teklay et al., 1998; Ayalew and Johnson, 2002; Tsige, 2006; Avigad et al., 2007), the ANS is made up of isotopically young crust with features including back-arcs, island arcs, and ophiolite-decorated sutures. The MB rocks differ from the ANS in that they have undergone longer-term, higher-grade gneissic metamorphism, dating back to orogenic events from the pre-Neoproterozoic (Stern, 1994; De Waele et al., 2006; Bingen et al., 2009; Fritz et al., 2013). Based on ‘crustal isotopic signatures’ in some ‘rocks’ from the ‘WES’, high-grade ‘gneissic’ rocks ‘sandwiching juvenile crust’, and spatial locations along ‘island-arc suture zones’, the presence of MB rocks in Ethiopia remains controversial (Ayalew et al., 1990; Ayalew and Peccerillo, 1998; Allen and Tadesse, 2003; Blades et al., 2015).

High-grade metamorphic rocks, metavolcanic rocks, metasedimentary rocks, and felsic and mafic intrusions are all found in the WES (Alemu and Abebe, 2000; Ayalew and Johnson, 2002; Allen and Tadesse, 2003; Alemu and Abebe, 2007; Woldemichale et al., 2010; Blades et al., 2015, 2017). These lithologic units were produced by 'subduction', 'intrusion', and 'metamorphism' during the 'collision' and 'crustal thickening' and are present in a number of 'accreted arc terranes' (Ayalew and Johnson, 2002; Woldemichale et al., 2010; Blades et al., 2015, 2017). All (apart from the really late incursions), according to Shelby Bowden et al. (2020), undergo metamorphosis. Prior to D2, a high-temperature gneissic to upper amphibolite facies event known as M1 took place. According to Ayalew and Johnson (2002), M1 was characterized by peak conditions of 600–800 °C and 5-8 kbar. 'Epidote and hornblende replacement products' show that M2 a low-temperature amphibolite facies, may have also involved aqueous fluids (Ayalew and Johnson, 2002). According to Ayalew and Johnson (2002) and Johnson et al. (2004), M2 was probably the product of late crustal thickening during D3.

The low-grade rocks of 'western Ethiopia' were correlated to the 'juvenile Pan-African assemblage' of 'northern Ethiopia' ('Adi Hageray', 'Adi Nebrid', and 'Adwa Block' of Tadesse 1996), Eritrea ('Augaro-Adobha Belt' of Ghebreab et al. 2009), and south-eastern Sudan, according to Tadese Alemu (2007), which was cited in Hamimi et al. (2021).

According to Abraham (1989), Gichile (1992), Tadesse and Tesfeye (1999), 'the basement geology' of 'southwest' Ethiopia and 'southeast' Sudan is made up of 'a number of' low-grade 'volcano-sedimentary belts' that are scattered with higher-grade gneiss terranes that, in some places, approach granulite facies grade. Ophiolitic-rich linear zones are typically found in the volcano-sedimentary belts. Examples include the Baragoi and Sekerr Complexes in northwest Kenya, the Adola-Moyale and Tulu-Dimtu Complexes in 'western' and 'southern' Ethiopia, and the Ingessana and Kabus Complexes in southeast Sudan. While parts of the interstitial gneiss terranes may be Palaeo- or Meso-proterozoic basements to the ANS, others may be Archaean in age and comprise a 'portion' of the Nile 'Craton'. Alternately, they might be 'remnants' of 'the Mozambique Belt', which are volcanic-sedimentary bands with unclear ages and structural links. Although dating has primarily focused on granitoids, U-Pb and Pb-Pb zircon dating (Ayalew and Gichile, 1990; Ayalew et al., 1990; Teklay et al., 1993; Ayalew, 1997) have not 'revealed' any pre-Neoproterozoic ages for these gneiss terranes. Recent U-Pb dating, however (‘eklay et al., 1998; Yibas et al., 2002) suggests that pre-Neoproterozoic zircon ‘xenocrysts’ were incorporated into some of the Neo-proterozoic ‘granitoids’ of ‘southern’ Ethiopia, which may account for an early pre-E EAO Rb-Sr metamorphic age of 1030 Ma discovered by Chater (1971) from Adole metasedimentary rocks. The Tuludimtu Orogenic Belt, a 200 km broad N-S trending zone next to the Sudanese border, is located in westernmost Ethiopia. It comprises of a volcanic-sedimentary package surrounded by gneisses of higher grade and has rocks in a linear zone with an ophiolitic affinity that is 20–30 km broad. The belt extends 500 km from north of the Blue Nile to south through the southwest Ethiopian regions of Gimbi-Assosa, Yubdo, and Gore-Gambella. Under Cenozoic cover, the belt is lost to the ‘north’ and ‘south’, although ‘the ophiolitic zone’ has been linked to the ‘Barka’ or ‘Baraka’ Suture in northwest Eritrea and the ‘Sekerr’ ophiolite in ‘northern’ Kenya (Berhe, 1990). Only a few local reconnaissance investigations have been done in the belt before; Examples are Kazmin et al. (1978); Davidson (1983); Abraham (1989); and Ayalew and Moore (1989). However, a more thorough investigation has just been carried out in the Baruda district, north of the Blue Nile, by Braathen and colleagues (2001). Teklay (1986) described the petrology of ‘the Tuludimtu Belt’ in ‘the Gore-Gambella region’ to the south, and Warden et al. (1982) specified the geochemistry of a few of ‘the ophiolitic’ rocks found within the Tuludimtu Formation. Chater (1971) also determined the ‘geochemistry’ and ‘geochronology’ of the Rb-Sr metamorphic age of 1030 Ma from Adole metasedimentary rocks.

Dereje Kenea (2017) indicated that The current studies have divided the tectonic ‘evolution’ of the ‘WES’ into the Gore-Gambella area which comprise ‘Birbir’, ‘Baro’, and ‘Geba’ domains (Teklewold Ayalew, 1997), and the Tulu-Dimtu belt which includes Aba Sena-Gimbi-Inango-Ayra transects and is formed by ‘Didessa’, ‘Kemashi’, ‘Dengi’, ‘Sirkole’, and ‘Daka’ domains from ‘east’ to ‘west’ (Allen and Gebremedhin Tadesse, 2003). According to Teklewold Ayalew and Peccerillo (1998), this classification is mostly based on the degree of metamorphism and lithological similarities found within the same domain. (Teklewold Ayalew, 1990: 1997; Allen and Gebremedhin Tadesse, 2003) divided the WES domains into different categories. The following describes these:

2.2.1 Birbir Domain

‘Plutonic’ and ‘volcanic’ rocks ranging from mafic to felsic are among the meta-sedimentary and meta-volcanic rocks found in the Birbir domain (Ayalew et al., 1990). According to Ayalew et al. (1990), the metasedimentary rocks include meta-greywacke, pelite, volcano-clastic, and carbonate rocks. The Birbir domain has foliated as a result of early shearing and syn-tectonic recrystallization, which may be related to the emergence of early folding (Teklewold Ayalew, 1997). The Birbir domain's structures, according to Teklewold Ayalew (1997), have the orientation of north-south striking foliations that dip sharply toward the west and stretching lineations defined by deformed clasts, minerals, and mineral aggregates that plunge 20° to the ‘north’ and ‘south’.

2.2.2 Geba Domain

According to Teklewold Ayalew (1997), the Geba domain has rocks including quartzo-feldspathic gneisses, medium grained ‘biotite’, and ‘hornblende-biotite’ gneisses. According to Ayalew et al. (1990), the gneisses in this region are migmatitic and contain lots of sub-concordant lenses made of granitic and pecmatitic elements. According to Ayalew and others (1990), the Geba domain's structures are distinguished by open D2 folding of the gneissic layering (S1) around gently descending NNE-trending axes and foliations that dip into the west direction.

2.2.3 Baro Domain

Garnet-sillimanite gneiss, calc-silicate gneiss with subordinate garnet-amphibolite, and magnetite-bearing quartzite are lithologic units found in the Baro domain (Ayalew et al., 1990). According to Teklewold Ayalew (1997), the Baro domain has linear features that are softly plunged to the north or south and planar structures that are oriented with a northerly strike and minor dips Eastward and westward.

2.2.4 Didesa domain

According to Allen and Gebremedhin Tadesse (2003), the Neo-proterozoic intrusive rocks poly deformed gabbroic and granitoid masses, post-kinematic mafic and felsic plutons, and moderate-grade para- and ortho-gneiss dominate the Didesa region. According to Tadesse Alemu and Tsegaye Abebe (2007), the banded mafic gneiss that makes up ortho-gneisses was created by a layered mafic intrusive body and comprises ultramafic bands. This domain contains the para-gneisses garnet-biotite gneiss, quartzo-feldspathic gneiss, and biotite-amphibole gneiss. According to Allen and Gebremedhin Tadesse (2003), the vast bulk of the lithologic units discovered in the Didesa domain is heavily foliated and have undergone extensive folding with numerous refolded folds indicative of poly-phase folding. The N-S trending Chugi Shear Zone serves as a tectonic boundary between this domain and the nearby Kemashi Domain towards the west (Allen and Gebremedhin Tadesse, 2003).

2.2.5 Kemashi domain

Kemashi domain is located ‘west’ of the Didesa ‘domain’ in ‘the west Ethiopian shield’. This domain encompasses lithological units such as; low-grade meta-sedimentary rocks like pelitic to psammitic schist, intercalated with chert, graphitic phyllite and marble and ultramafic–mafic meta-volcanic rocks such as serpentinite, talc-chlorite–tremolite schist, meta-basalt, talc schist, talc-carbonate schist, and pyroxenite (Allen and Gebremedhin Tadesse, 2003). According to Allen and Gebremedhin Tadesse (2003), rocks within this Domain are highly deformed and sheared. Small-scale, westerly-verging, tight to open, and recumbent Meta-sedimentary unit bedding frequently exhibits F1 folds. (Allen and Gebremedhin Tadesse, 2003; Tadesse Alemu and Tsegaye Abebe, 2007). Contact between the Kemashi Domain and adjacent terranes are tectonic contact of N–S orientation of the Beleke Shear Zone (Allen and Gebremedhin Tadesse, 2003).

2.2.6 Dengi domain

West of the Kemashi Domain is where this Domain is located. According to Allen and Gebremedhin Tadesse (2003), the Dengi domain is made up of deformed and metamorphosed volcanic-sedimentary sequences such meta-basalts, meta-andesites, meta-rhyolites, phyllite, garnet mica schists, marbles, meta-gabbros, amphibolite, and meta-granitoids. According to Allen and Gebremedhin Tadesse (2003), the epidote-amphibolite facies metamorphic conditions led to the metamorphosis of the rocks in this region. The tectonic contact exists between the ‘gneisses’ and the ‘volcano-sedimentary sequence’. According to Allen and Gebremedhin Tadesse (2003), the sinistral NW moving Chochi Shearing Zone has been ‘linked’ to the foliation trend within this domain that shifts from N-S to NW-SE.

2.2.7 Sirkole domain

The Sirkole Domain is situated in the Tulu Dimtu belt's northwest and stretches all the way to Sudan. The rock units that make up the Sirkole domain, according to Allen and Gebremedhin Tadesse (2003), include mafic to felsic meta-volcanic rocks intruded by deformed and undeformed granitoid plutons, low- to moderate-grade meta-sedimentary rocks, and moderate-grade poly-deformed gneisses. According to Allen and Gebremedhin Tadesse (2003), amphibolite facies assemblages are present in both the ‘gneiss’ and the ‘volcano-sedimentary’ successions in this region, indicating the Grade of metamorphism there. According to Allen & Gebremedhin Tadesse (2003), the volcano-sedimentary succession in the Sirkole domain is assumed to be folded and strongly cleft, with an N-S striking, easterly dipping schistosity and a mineral extending lineation gradually sloping eastward.

2.2.8 Daka domain

This territory borders Sudan and is located in the southwest portion within the Tulu-Dimtu belt. According to Allen and Gebremedhin Tadesse (2003), “the Daka domain” is ‘made up of’ lithological units with high-grade rocks such moderate-high grade poly-deformed gneisses and granitoids that are intruded upon them. According to Tesfaye Kebede and Koeberl (1999), the gneissic rocks of the Daka Domain can be classified into three lithological units. The Tosho Gneiss and the Yangu Granitoid Gneiss, two of the units, are ‘associated’ with the two gneissic units of the Sirkole Domain. A granulite facies unit with banded ortho-pyroxene makes up the third gneissic unit in the Daka Domain. The Shear zone in Yangu, which cuts through this domain's northwest region to the north along the Daka River's Thrust and is primarily made up of the Yangu Granitic Gneiss, is a dextral NE-SW trending shear zone in the Daka Daomain.

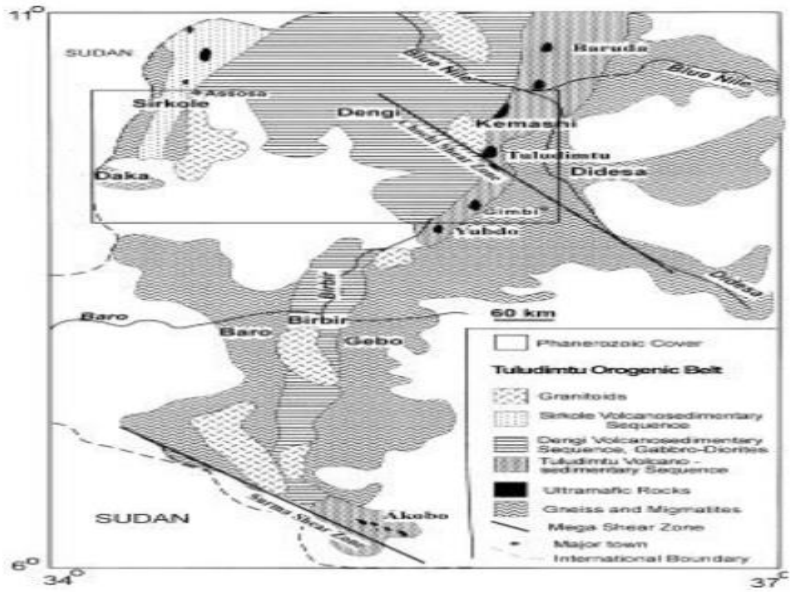

Figure 5: The Geological map of Tuludimtu Belt in western Ethiopia

(Allen and Gebremedhin Tadesse, 2003)

According to Tadese Alemu (2007) as in Hamimi et al. (2021), Western Ethiopian Precambrian could be split into three terranes that are inclined north to south that are separated by noticeable shear belts based on a combined perspective of Petrology, geochronology, lithology, and structure. The Asosa terrane, which is made up of several volcanic-sedimentary sequences and gneisses, Nejo terrane, which is primarily made up of meta-volcanic and meta-sedimentary suites, and the Gimbi terrane, which is distinguished by the presence of gneisses-migmatites and meta-volcano-sedimentary suites, are among them. Asosa and Nejo terranes are divided by the Sirkole-Birbir Shear Zone, and Nejo and Gimbi terranes are divided by the Shear Belt of Tulu Dimtu-Baruda-Akobo. Tadesse Alemu (2007) divided the region's lithology into the following categories to define it:

a) Gimbi Terrane

Two general categories can be used to categorize the Gimbi terrane east of the Tulu Dimtu-Baruda Belt (TDBB): interaction between gneiss and migmatites and (ii) volcano-sedimentary sections. Strike-slip shearing marks the boundary between the gneisses and the metavolcano sediment. Four lithological domains represent the gneiss and migmatites. These are (i) the Dura domain, (ii) the Didesa domain, (iii) the Geba domain, and (iv) the Hamar domain, listed from north to south.

The Didesa domain and the NE-trending dextral strike-slip Beko Abo-Guch and Guttin shear zones border the Dura domain to the east and the south, respectively. It is primarily composed of gneisses, migmatites, and amphibolites, which are high-grade rocks. Most of the gneisses are granitoid gneisses, with biotite gneiss and biotite-hornblende gneiss occupying minor positions. On a new outcrop, the granitoid gneiss is typically medium to coarse-grained with a pinkish color (occasionally fine-grained variations appear when it is strongly deformed or sheared). It is often homogeneous in terms of both texture and mineralogy. Pegmatite veins of varied thicknesses and generations (deformed and undeformed) penetrate through it.

Gneiss and granulite that has been severely deformed, recrystallized, and in some cases partially migmatized make up the Hamar domain (Davidson 1983), which covers a large portion of the Gimbi terrane's southern region. Five main lithologies were noted by Davidson (1983). Mafic hornblende gneiss and amphibolite are among them, as are well-layered biotite gneiss with discernible meta-sedimentary components, predominantly grey biotite-hornblende gneiss of variable color index, partially containing ill-defined masses of relatively uniform ortho-gneiss of grano-dioritic, tonalitic, and dioritic composition, pale-pink to light-grey quartzo-feldspathic While locally undergoing granulite facies metamorphism, all of these rocks are mostly subjected to amphibolite facies.

Four domains correspond to the meta-volcano-sedimentary sequences found in the Gimbi Terrane. These are the Anja domain, Shar domain, Kemashi domain, and Akobo domain, in that order. According to Seyid (2002), the ‘northern’ portion of the meta-volcano-sedimentary sequences is covered by the Anja domain. The domain, according to Seyid (2002), is made up of marble and undifferentiated meta-volcano-sedimentary rocks. The domain is mosly made up of undifferentiated meta-volcano-sedimentary rocks, which can be divided into varied ratios of mica schist, hornblende schist, feldspar-quartz schist, chlorite schist, quartzite, and phyllites. The marble exhibits a variety of colors, including white, light grey, grey, and dark grey, and is found surrounded by basic and ultrabasic rocks. Although medium to coarse grained locally, it is typically fine to medium grained.

Meta-sediments, ultra-mafics, and meta-volcanic rocks are the primary rock types in the Shar domain (Tsige 2008). The meta-sediments include chert, marble, phyllites, graphite schist, psammo-pelitic schist, quartzite, and quartzite with graphite. With these meta-sediments, ultra-mafic rocks are closely related.

b) Nejo Terrane

The Nejo Terrane has a wedge-shaped map contour that is 'narrower' in the south and 'wider' in the north. Further south, the wedge is truncated by a NW-trending Surma shear zone. The Sirkole 'shear zone' (SSZ) and TDBB form the terrane's western and eastern boundaries, respectively, with the Asosa terrane serving as the terrane's middle boundary. The shear zone of Debdeba, which shares Gimbi terrane with Nejo terrane to the east, marks the northern boundary between the two terranes.

There are four lithological domains in the Nejo Terrane. These include the domains Guba-Beles, Gesengesa, Katta, and Birbir. The Guba-Beles domain, which was formerly known as the Guba domain and the Beles domain, makes up the northern portion of the terrane (Seyid, 2002). The five lithological 'units' that 'make up' the 'rock' types in the 'Guba-Beles' domain are (i) the Diopside-Hornblende Gneiss, (ii) the Biotite and 'Biotite-Hornblende' Gneiss, (iii) the Migmatitic Gneiss, (iv) the Meta-Sediments, and (v) the Marble (Seyid 2002). The Gesengesa 'domain', also known as the Gesengesa 'schist' and gneisses (Tefera 1991) and 'Chochi domain' (Alemu and Abebe 2000), is 'made up of' a variety of rock types, including garnet-mica schist, biotite-kyanite-quartz schist with subordinate graphite schist, quartzite, 'marble', and amphibolite. There are numerous locations where the aforementioned rock types are in tectonic contact with minor lenses and 'pods' of mafic-ultramafic rocks.

c) Assosa Terrane

Along with the 'Nejo terrane', the 'Assosa terrane' is bordered to the 'west' by the Sirkole 'shear zone' (SSZ) and the 'Birbir' shear zone. Covers made of Phanerozoic rock conceal the terrane's southern extension. The Surma shear zone, which has a NW trend, is juxtaposed with the Nejo terrane further south. The two main categories are gneissic association and meta-volcano-sedimentary sequences. A pair of lithological domains makes up the meta-volcano-sedimentary sequences. This includes (i) the Afa domain and (ii) the Dul domain. In the Afa domain, three lithological units have been recognized. According to Alemu and Abebe (2000) these are: (i) Greenschists, (ii) Quartz-graphite schist, and (iii) Biotite-feldspar-quartz gneiss. The Dul domain is marked for a range of volcanic-sedimentary lithological units metamorphosed to the greenschist facies, associated with mafic-ultramafic rocks, and granitoid intrusives (Ahmed 1982; Abnet 1989; Negussie 1988; Wollie Sheka et al. 1990; Mersha et al. 1995; Bekele 1999; Guliev 1982; and Soukhoroukov 1980)). The Asosa-Kurmuk Belt was the previous name for the mafic-ultramafic assemblages found in the Dul domain (Alemu and Abebe 2000). The Asosa-Kurmuk belt divides low-grade meta-volcano-sedimentary sequences to the 'east' from high-grade 'gneiss' (Kurmuk gneiss) in the 'west'. Meta-volcano-sedimentary 'sequences' and 'linear' but 'discontinuous bodies' of mafic-ultra-mafic rocks that appear at Mt. Dul, Azale-Akendeyu, and Gizen are representative of the belt. According to Zuber (1986) and Abnet (1989), the mafic-ultra-mafic occurrences on Mount Dul are a component of an ophiolitic succession. A feature known as 'the Ingessana-Port Sudan suture zone' was identified by regional 'correlation' of the Mt. Dul 'ophiolites' with the 'Ingessana' and Port Sudan 'ophiolites' in 'north-eastern Sudan' (Berhe 1990). Four lithological domains in 'the Assosa terrane' represent the gneissic relationship. These are (i) the Kurmuk domain, (ii) the Daka domain, (iii) 'the Baro domain', and (iv) the Surma domain. Strike-slip shearing with a NE trend indicates the interaction with 'the volcano-sedimentary assemblages'. Grey, medium to coarse-grained, hornblende-biotite gneiss with well-banded biotite is known as the Kurmuk domain, also identified as 'the Kurmuk gneiss' (Tefera, 1991). It has pegmatitic and migmatitic features. and granitic mobilization of 10–20%. The banding, which is distinguished by alternating layers rich in quartz-feldspar, hornblende, and biotite, can be millimeters to centimeters thick. It happens frequently for banded granitoid rocks to become homogeneous.

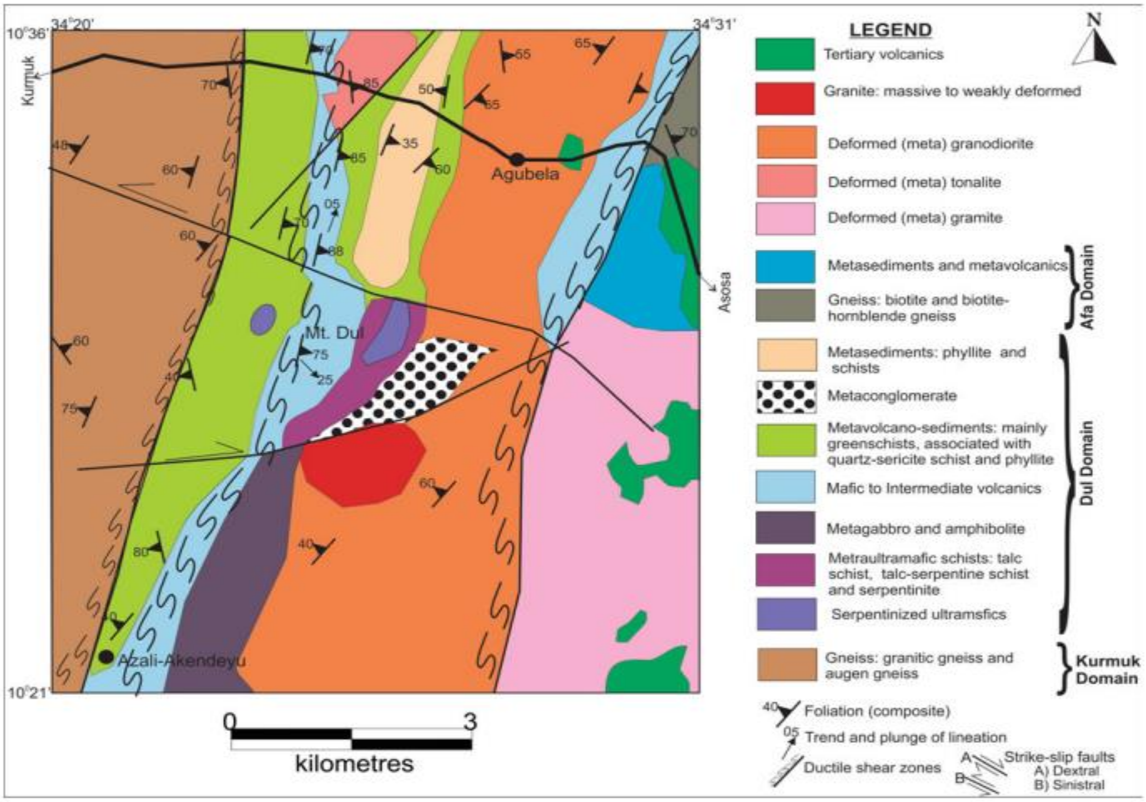

Figure 6: The Map of Dul's geology and the surrounding territories (adapted from Wollie Sheka et al., 1990; Mersha Jembere et al., 1995 as in Zakaria Hamimi et al., 2021)

The Kurmuk domain borders the E-W trending structures that make up the Daka domain, which 'Allen and Tadesse (2003)' refer to as the Daka thrust. However, Phanerozoic cover rocks hide its southern continuation. 'Gneissic rocks' which are separated into 'three lithological units' make up the majority of the structure.

CHAPTER THREE

Materials and methodology

This study applied a quantitative technique. The quantity of various samples and the geochemical analysis of whole silicates serve as a representation of the area in question. Based on the percentage mineralogy, petrographic study also establishes the lithological units. The lithological ‘units’ of the studied region are primarily the ‘focus’ of this ‘investigation’. Additionally, details regarding the physiography, climate, and settlements of ‘the research area’ are gathered with special care paid to the representativeness of the samples and the reliability of the data. The sampling method that was used in this ‘study’ is random sampling during field trips. For the successful completion of this work, a field trip was conducted for the collection of samples. Samples were collected from different exposures. Nine representative samples were selected for petrographic and complete silicate geochemical analysis at the Mekanissa branch of the Ethiopian Geological Survey Institution. The petrographic microscope at the Addis Ababa University ‘School of Earth Sciences’ petrographic lab is used to examine the thin section. For the pictures and more detailed feature information, I employed both plane polarized light (PPL) and crossed polarized light (XPL). Different techniques, such as LiBO2 fusion, HF attack, gravimetric, colorimetric, and AAS, are used to prepare geochemical data. Using LiBO2, the sample is mixed with the flux and heated to high temperatures to melt the sample and dissolve the minerals. The resulting liquid is then cooled and dissolved in an acid solution for analysis. This allowed for the determination of major elements in silicate rocks using Atomic Absorption Spectroscopy (AAS).. For the breakdown of silica and other silicates, HF attack was used. Based on the solid's mass, a gravimetric examination was done to determine the concentration of main oxides. With the help of a color reagent, the colorimetric approach was used to calculate the chemical compound concentration in a solution. Quantitative analysis of chemical compounds by ‘free atoms’ in the ‘gaseous’ state, was done using atomic absorption (AAS). The technique is ‘based’ on the finding that when an element is atomized, its atoms can absorb electromagnetic radiation. The reduction of response in a detector caused by atomic absorption during the atomization of a sample in a laser beam can be calibrated and is sensitive at the ppm level (Price, 1972). The values were compared to the geochemical reference materials to determine the accuracy.

Equipment used

Throughout the journey, various pieces of geological field equipment were utilized for the collecting of trustworthy and representative fresh samples. These include the tools that were 'used' in the field to gather, measure, and record samples during field trips, such as the GPS, topographic map, geological hammer, sample bag, digital camera, pencil, field notebooks, markers, and pens. Geochemical classification diagrams were plotted using the GCDkit software. The study area's imagery was downloaded using the Open Topography and Google Earth Pro programs. ArcGIS technology was used to produce a lithological map of 'the research area'. Three distinct procedures, the pre-field, field, and post-field procedures, were used to collect the data. Pre-field: Various earlier studies that are 'relevant' to this particular study were gathered and reviewed from published and unpublished papers, maps, journals, scientific publications, and websites. Fieldwork: The collection of representative, fresh rock samples, in addition to thorough descriptions of the hand specimen and exposure scale of the local rock units. The fieldwork also included reading GPS coordinates and taking pictures. The following provides a 'summary' of the research's methodology.

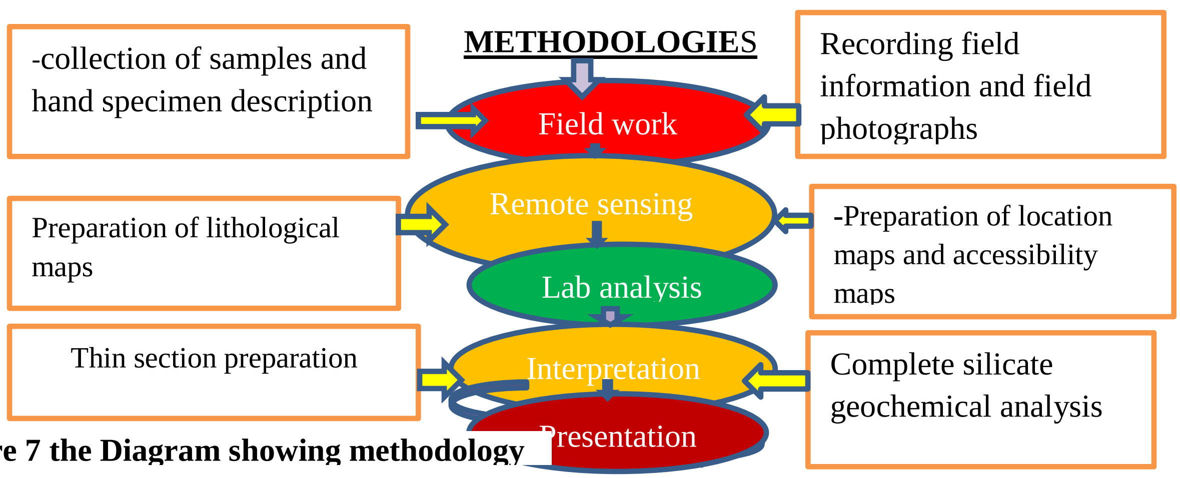

Figure 7 the Diagram showing methodology

CHAPTER FOUR

LOCAL GEOLOGY OF 'THE STUDY AREA'

According to Tadesse Alemu's categorization of the Tulu-Dimtu belt in 2007, the study area is 'located' in the Dul domain of the Assosa Terrane. The study region revealed rocks at various locations, including hill, mountain, river, and road cut exposures that varied in color, grain size, and texture. The following is how these exposures are presented:

4.1 Massive Basalts

Greenish-black, fine to medium-grained, massive rocks at Mount Dul-Undu have been identified in the field as massive basalts. These rough rocks have a reddish 'wheathered' color. The ridges at Mount Dul Undu and its surrounds are mostly made up of this 'type' of rock. The fine-grained white chalky material can be seen as a vein in the metabasaltic groundmass on the flat areas surrounding Mount Dul Undu (fig. 8c). The rocks 'referred' to in the field as basaltss are described as having fine-grained rocks with a deep black color. By way of road cuts, these rocks are mostly exposed at high topographies and rarely on flat topographies.

Figure 8: massive basalts: a, the field photograph at Mountain Dul Undu b&c the field photography of volcanics and chalky rocks appeared as a vein in volcanic groundmass at a road cut exposure on the flat topography around the Dul-Undu Mountain.

4.2 Quartz infill

There is quartz infill seen in the amygdaloidal basalts. The amygdaloidal basalt revealed on the study area's flat terrain is primarily found around mountain Dul Undu near Famestere village in the Kurmuk area. Greenish and red-colored minerals, most likely the result of alteration, can be observed filling the spaces in the rock along with the infilling quartz.

Figure 9: quartz infill seen on the amygdaloidal basalts s in 'the study area' (from field photograph)

4.3 Jointed basalts

Basalt is covered by light-colored rock at the quarry site close to the 'main' asphalt road around Mount Bilbilo in Bamadon Village. The exposed rock that covers the basalt at the quarry site exhibits some stratification. The basalt close to the layered rock has extensive weathering. Basalt displays two joint sets that are slightly offset from the stratified rock. Rhyolite, which is the rock overlying the basalt and is found in the areas close to the two high ridges of Undu Mountain, has been identified through geochemical analysis.

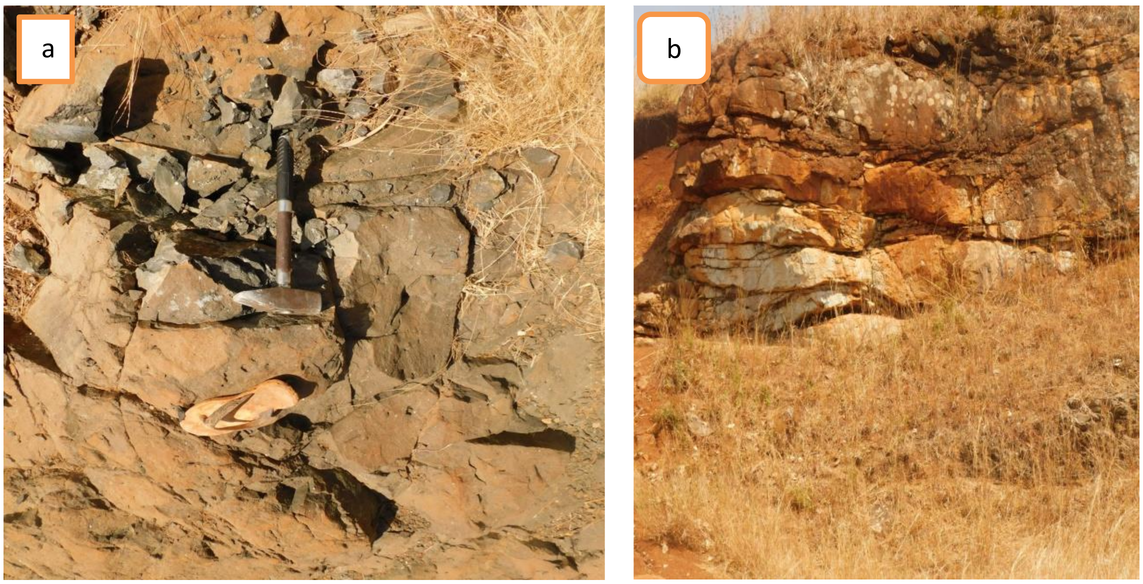

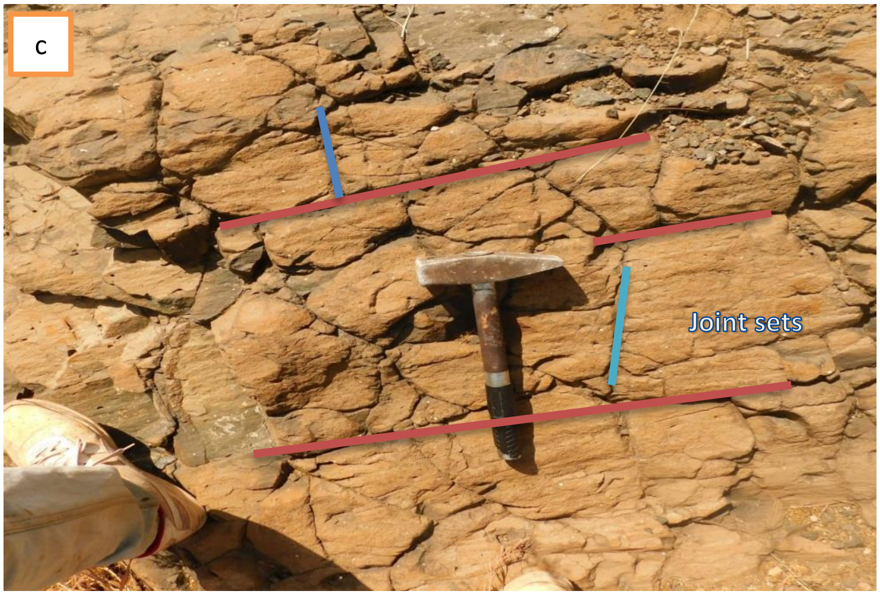

Figure 10: Wheathered basalts with rhyolites: a, wheathered basalt b, the layered rock that overlying it determined geochemically as a rhyolite and jointing in basalt near Bamadhon village of Homosha woreda

The flat landscape that surrounds Undu Mountain is also composed of black, fine-grained basaltic rock that is not weathered. The flat lands surrounding Homosha town and its environs were where the unweathered basalt was discovered. Fine to medium-grained basaltic rock surrounds Homosha town, making it possible to see the light-colored minerals there with the naked eye.

Figure 11: Unweathered basalts; a, around Homosha, b, near Undu

4.4 Rhyolites

As we approach Undu Mountain, the white, fine-grained rock is revealed on the slopes and forms the two ridges from the base to the summit. According to geochemical analysis, this rock is rhyolitic since it contains 78% silica on average. This rock also formed the Gule Mountain and its environs near Famestere village and occurred as an intercalation and overlain a basaltic rock near Bamadhon village.

Figure 12: Rhyolitic exposures in 'the study area'; a, the smooth whitish rock at the foot and b, at the top most of Undu Mountain.

4.5 granitic rocks

Medium to coarse-grained granitic rocks with predominately pinkish minerals make up the other ridges of Undu Mountain. Quartz, k-feldspar, and biotite minerals are 'observed' in the coarse-grained granite with the naked eye. The black-colored, fine-grained rock, which is intercalated with granitic rock and becomes visible on a very tiny scale as we travel away from the granitic exposure toward the valley (this rock sample has been identified as granite by geochemistry!), is uncovered as we move away from the granitic exposure. As we go away from Undu Mountain, certain surface features may be seen on the granitic rocks. These features include tiny quartz veins and tiny ring-shaped formations that might be thought to be the remains of animals or the long-term effects of rain.

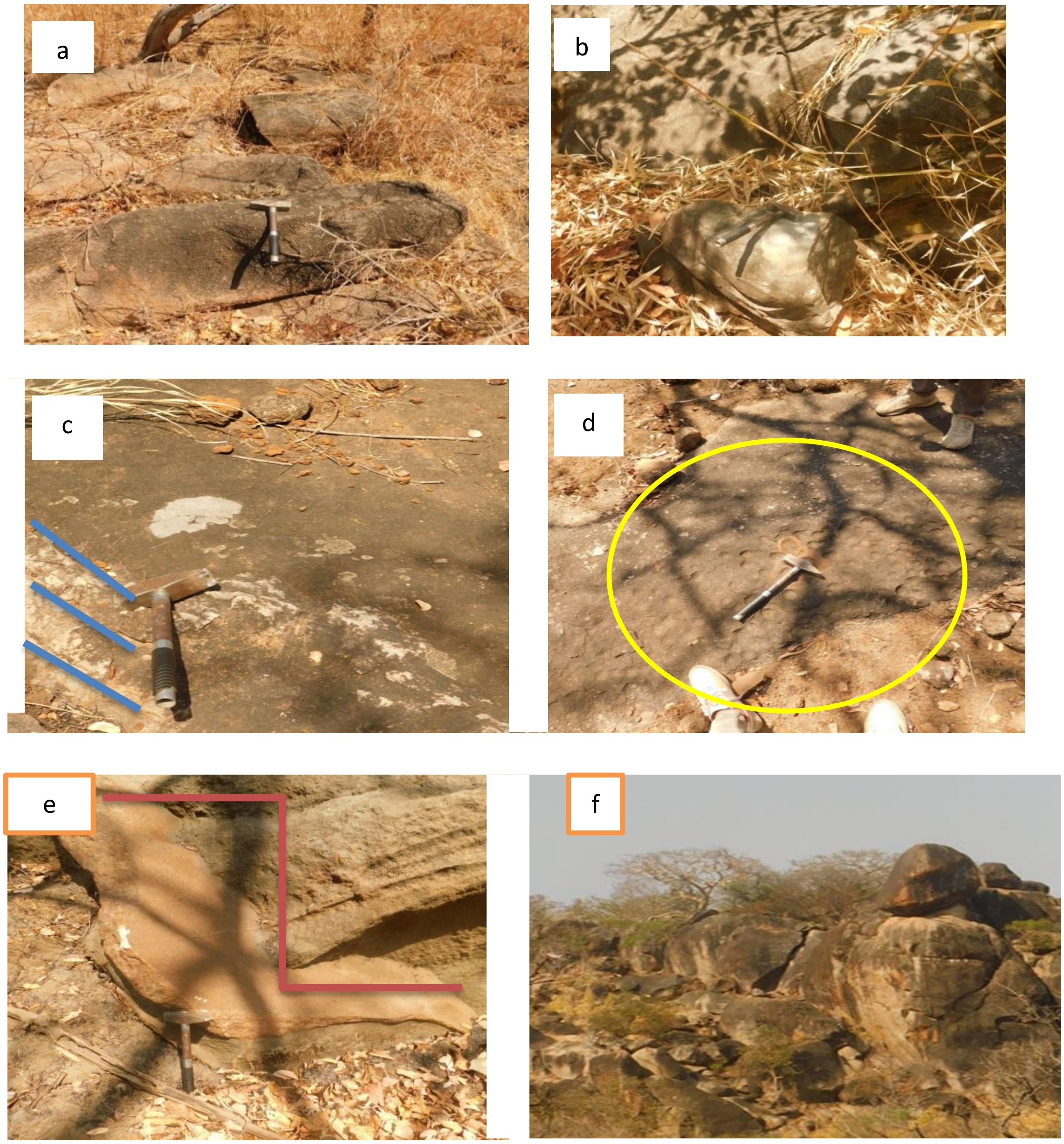

Figure 13: granitic exposures; a, coarse grained granite, b, fine to medium grained granite, c, small quartz veins on granite, d, circular structures, e, granitic intergrowth, and f medium to coarse grainedgranitic outcrop away from Undu Mountain.

4.6 Diorite

The road cut in the 'area' of Genze-Fuulu, which is close to Bibo Mountain, exposes the medium to coarse-grained rock that is 'dominated' by quartz and biotite. Geochemical analysis confirms that the rock is diorite. As we near the exposure of the granitic rock, this rock is becoming finer.

Gnesosity can be plainly seen at the granitic contact. The granite's contact point exhibits significant deformation. The granitic rock exposed near Biibo Mountain with this rock is pinkish in color and has various colors and grain sizes when compared to that of Undu Mountain. The major mineral appears to be k-feldspar, which is extremely coarse-grained.

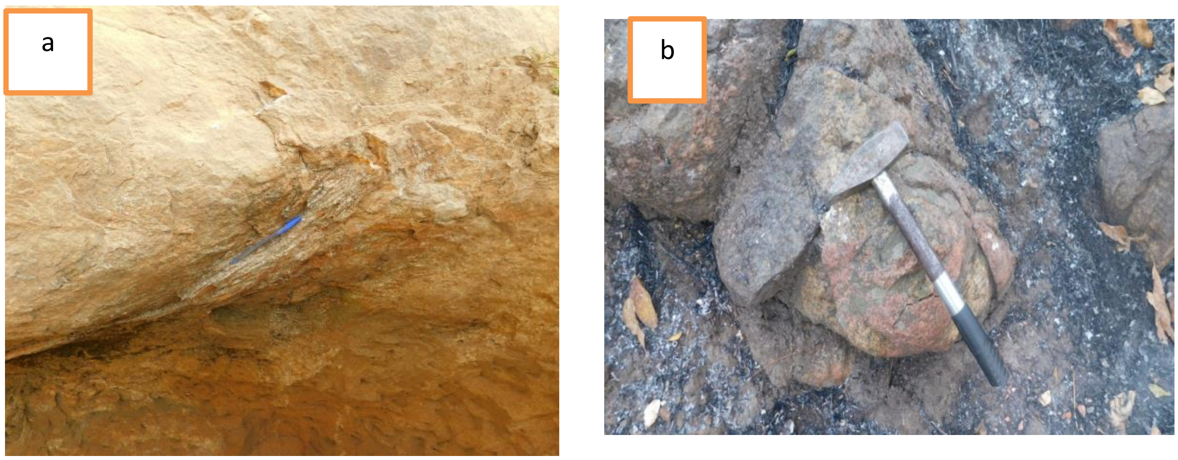

Figure 14: a) the 'contact' between the granite and the quarts and biotite dominated dark greenish rock (diorite), b) the pinkish colored granite.

4.6 Quartz vein

In the consolidated earth materials close to the Shenga fall in the Homosha district, a vein of white quartzite with a maximum thickness of one meter is visible. Comparatively speaking, it is thicker and clearer than the quartz veins and precipitates that can be found nearby Mount Dul Undu and at Undu Mountain

Figure 15: quartz vein observed in the area of study

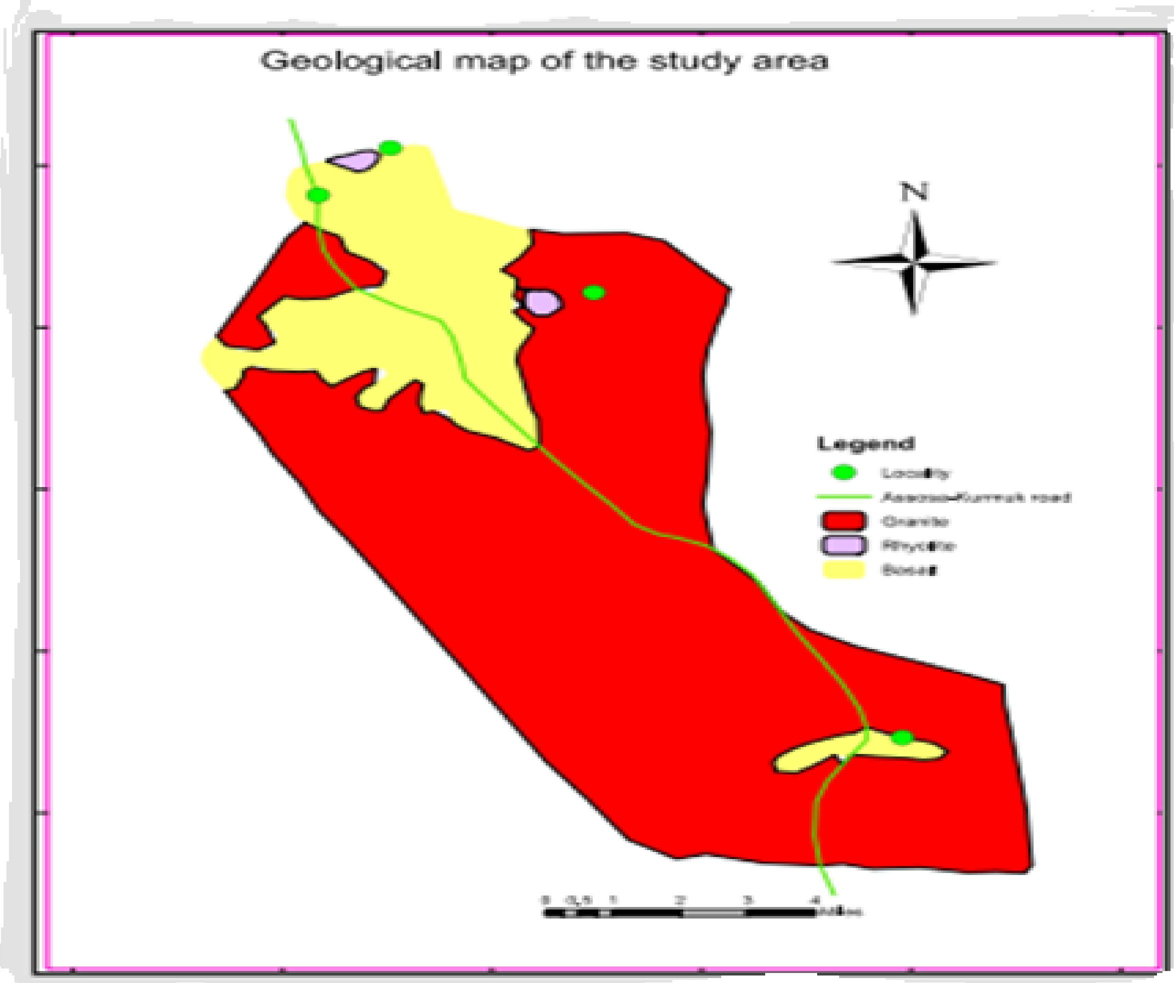

Figure 16: The geologic map of the study area

T

CHAPTER FIVE

PETROGRAPHY OF 'THE STUDYAREA'

At the Geological Institute of Ethiopia's Mekanissa branch, the nine (9) representative rock samples that best represented the rock type were chosen for petrographic study. At Addis Ababa University's 'School of Earth Science', the samples were processed and subjected to petrographic analysis. The results are summarized below;

D2S1 (Aphiric Basalt)

The groundmass of Sample D2S1 is mainly colorless plagioclase laths. This rock was collected from the Mountain Dul Undu region close to Famestere village. Rarely are the big and twinned plagioclase feldspar crystals visible as phenocrysts in the smaller laths. This thin section contains a plagioclase phenocryst that shows zoning due to variations in the shade of grey interference color, which signify distinct extinction positions for various crystallographic regions. Clinopyroxenes with vivid yellow colors are seen in the thin section. Between the plagioclase elongated crystals, there are smaller amounts of biotite and olivine grains. This sample thin section contains opaque minerals in the groundmass as well, which display dark color under both XPL and PPL lights. These euhedral/cubic opaque crystals can be identified in this thin section image and could represent iron oxide minerals like magnetite because of their general opacity.

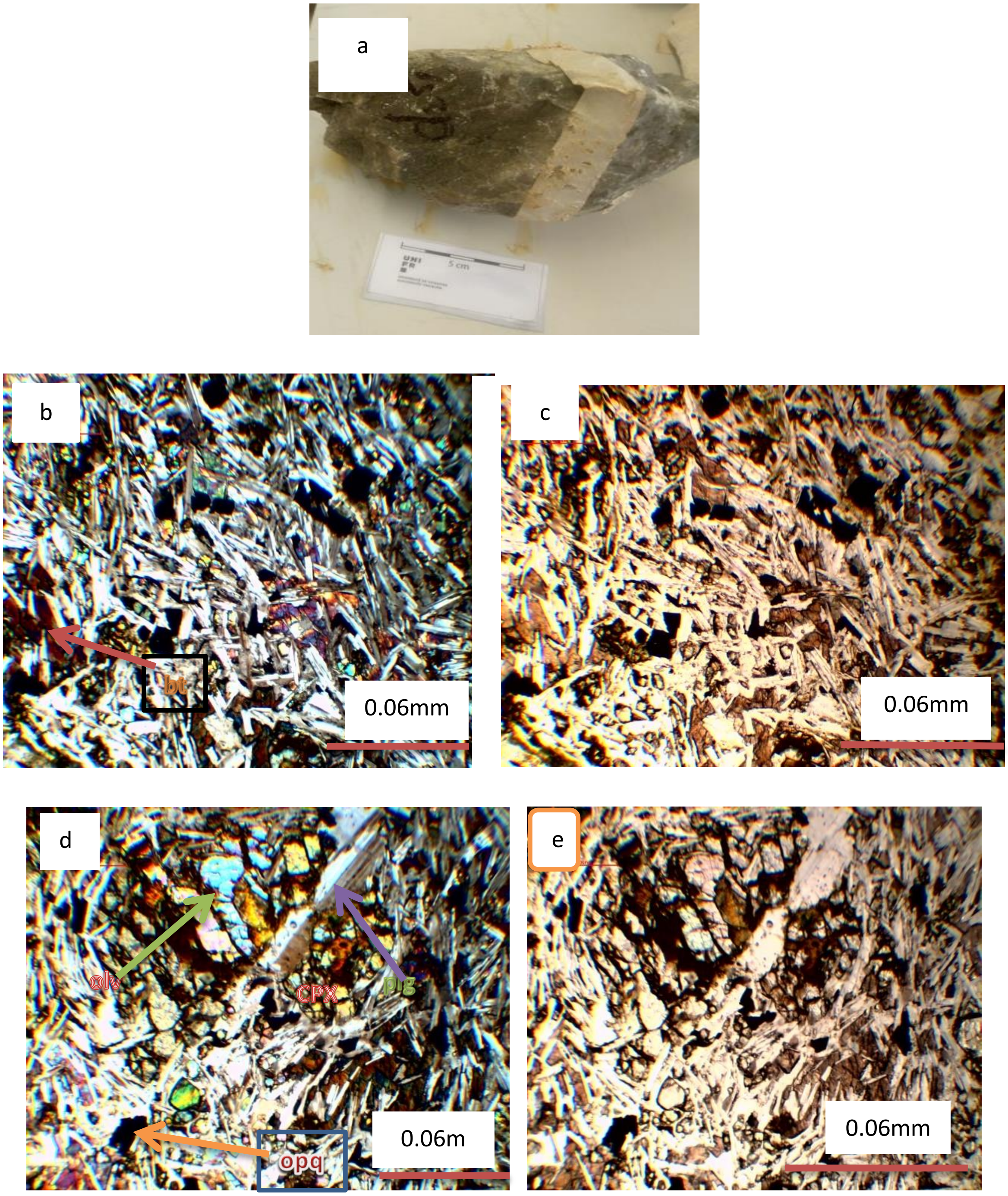

Figure 17: sample D2S1; a, hand specimen, b&c shows the general XPL and PPL views of the thin section, while d&e shows the XPL and PPL of the observed minerals respectively.

D1S1 (crystalline Basalt)

It is discovered that Sample D1S1, which was likewise obtained on the Dul-Undu Mountain, contains plagioclase crystals that are well-developed and have a very evident polysynthetic twinning. The plagioclase crystals typically align in a sub-parallel pattern. Between the plagioclase crystals in this sample's thin section are olivine crystals. High relief and some good cleavage-like structures are present in the olivine crystals, along with a variety of irregular cracks. In XPL, several interference colors are displayed. This could be resulting from the 'fact' that they show various crystal cutting orientations. It is found that 55% of the detected minerals are plagioclase, 40% are olivine, 3% are hornblende, 1% are pyroxene, and 1% are opaque minerals. It is determined that the rock is Basalt.

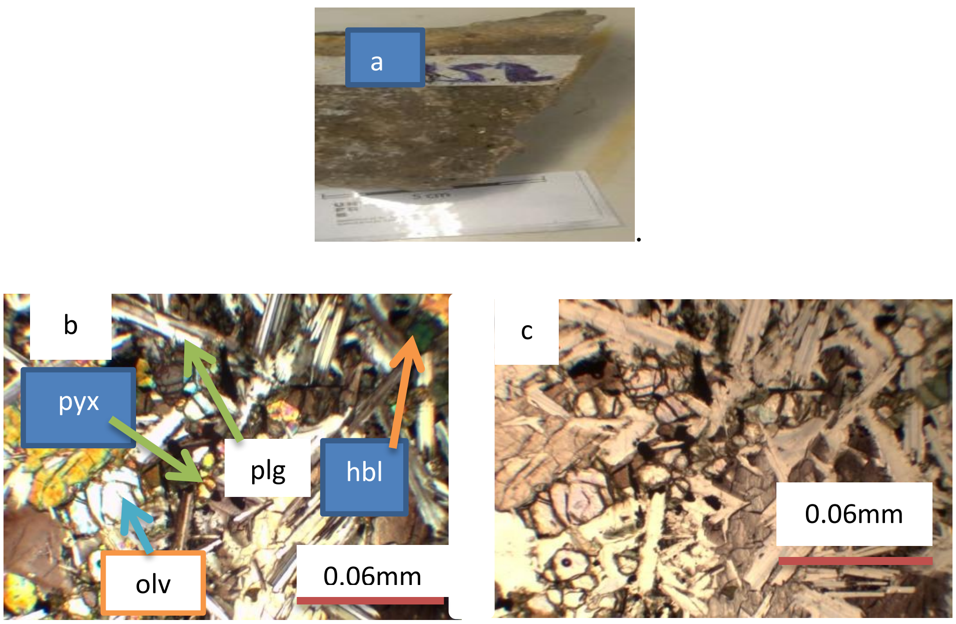

Figure 18: hand specimen and micro-photography of sample D1S1; a, hand specimen; b, XPL view and c, the PPL view of the sample thin section D1S2 collected from Dul Undu Mountain.

D3S1 (phyric basalt)

Plagioclase crystals that display polysynthetic twinning makes phenocrysts of Sample D3S1's structure. Additionally, pyroxene crystallized in the fractures of olivine phenocrysts that took the shape of euhedral hexagons. Fine-grained plagioclase laths make up most of the groundmass, but there are a ‘few’ opaque minerals present as well. Observed in this sample is the intergrowth of pyroxene on olivine. High relief can be ‘seen’ in the olivine crystals, which also exhibit a number of irregular crack patterns. In XPL, several interference colors are displayed. This could be resulting from the ‘fact’ that they show various crystal cutting orientations. 50% plagioclase and 50% olivine make up the phenocrysts.

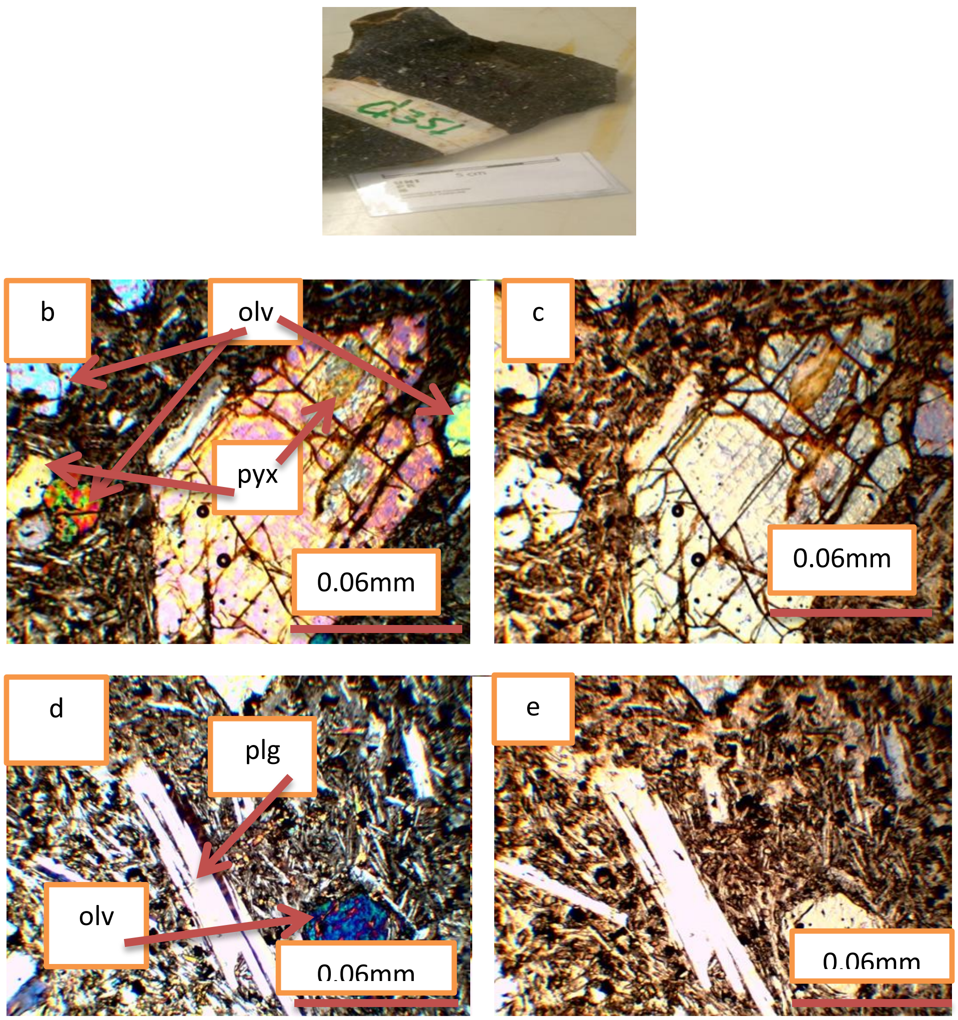

Figure 19: hand specimen and micro-photography of sample D3S1; a, hand specimen, b&d XPL, c&e, PPL

D2S2 (amygdaloidal basalt)

The vast majority of precipitating minerals in the D2S2 sample, which was gathered from the flat areas surrounding the peak Dul-Undu, are surrounded by other minerals that range in color from yellowish to reddish. High pleochroic minerals surround the quartz precipitates in a reddish color. After mineral precipitation, they are likely clay minerals that filled the pore spaces together with quartz. When the petrographic microscope's stage is rotated, they turn from reddish to pink in color. ‘Most’ of the minerals seen are quartz. This rock's thin-section also shows crystals of altered olivine and plagioclase. Most of the grains has a subhedral to euhedral form and is elongated. Geochemical classification designates the rock as basalt. During the field description, it is also determined to be amygdaloidal basalt.

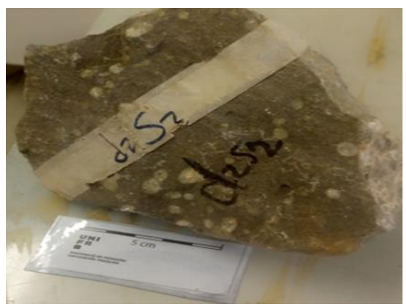

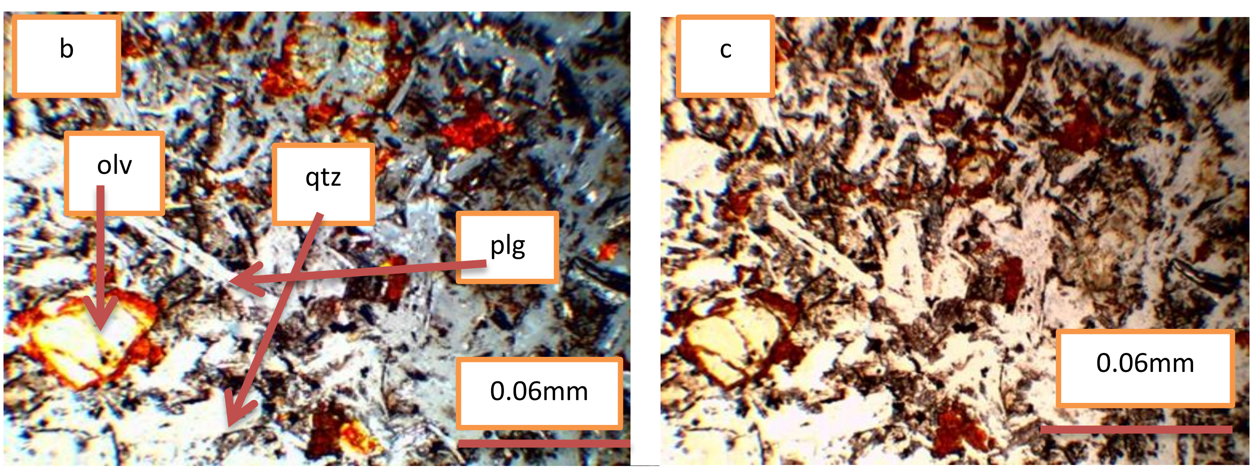

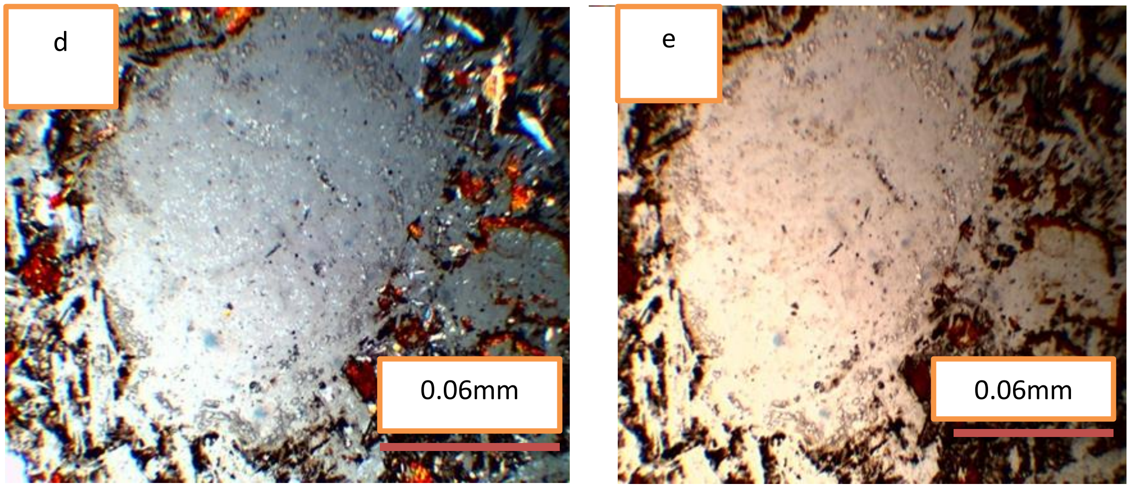

Figure 20: hand specimen and microphotography of sample D2S2; a, hand specimen;b&d shows different views of D2S2 in XPL while c&e& shows PPL views of the sample.

D2S5 and D3S2 (Rhyolites)

Very fine-grained colorless to whitish minerals that crystallized in a very fine-grained groundmass make up Sample D3S2. The main minerals in this sample are quartz and feldspar. Additionally, a minor amount of biotite is visible. When the microscope stage is turned, the extinction of these fine-grained feldspar minerals is seen. Mineral inclusions ranging from colorless to white are present. This rock sample was found to have a ‘significant’ number of contaminants, which appear as tiny black spots. It is discovered that Sample D2S5, which was taken from the quarry site next to Mountain Tinishu Bilbilo in the village of Bamadhon, has a felsic mineral with impurities. Rhyolite is the designation given to this rock by TAS geochemical classification. This ‘suggests’ that the feldspar and quartz minerals, which make up this entire thin section, are the impurity-containing minerals. The exceptionally clear and white interference colors of the quartz minerals set them apart from the feldspars. The feldspars in this thin section have undergone significant alteration.

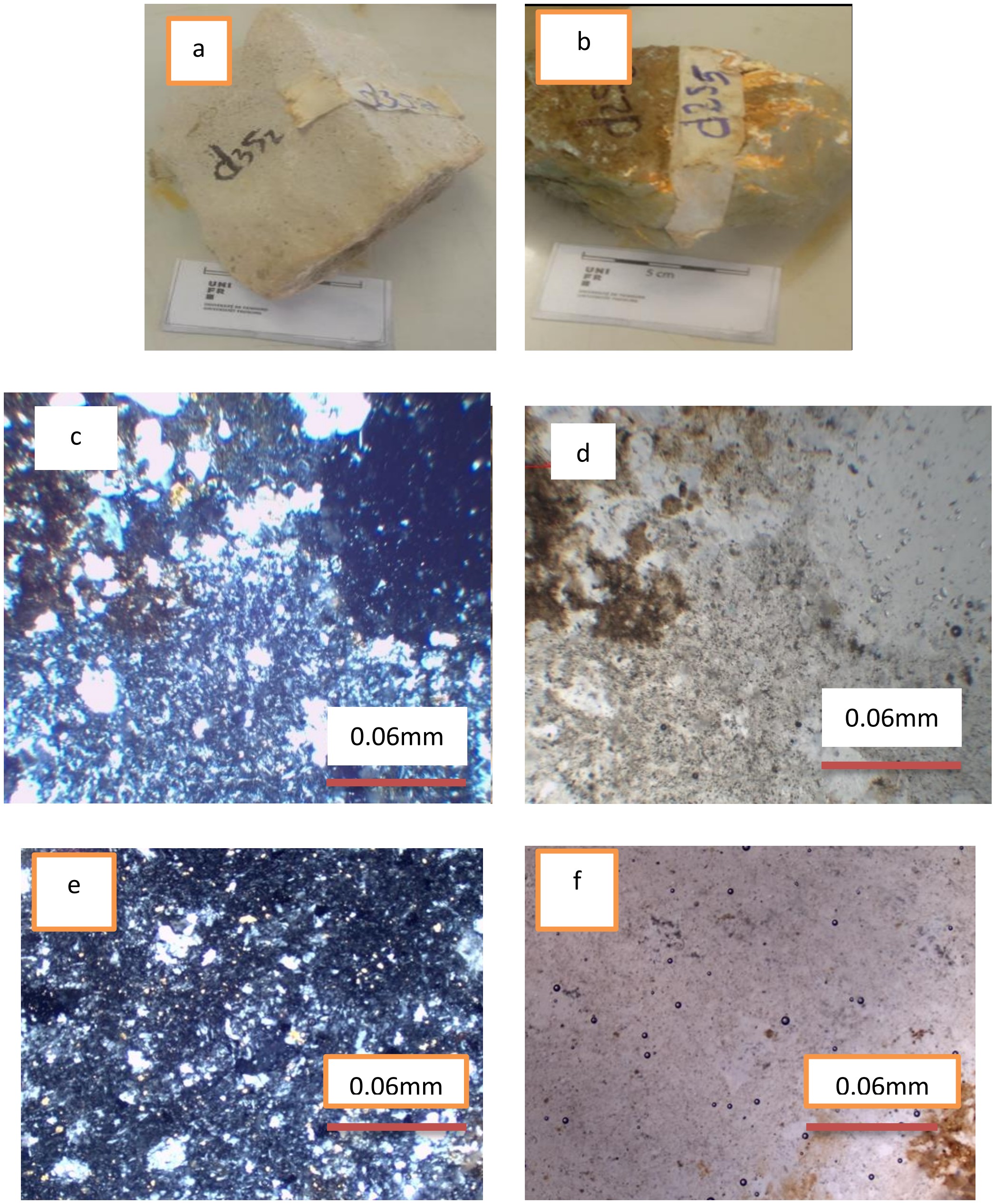

Figure 21: hand specimen and micro-photography of samples D3S2 and D2S5; a&b, hand specimens; c&e, XPL and d&f, PPL views of samples D3S2& D2S5 respectively.

D3S7 and D4S1G (Granites)

Sample D3S7, which was gathered near Undu Mountain, has feldspar and quartz minerals that have undergone extensive fracture. The colors of the quartz and feldspars range from colorless to bright white. They combine to form crystals that range in shape from subhedral to euhedral. The quartz crystals have very white interference color, undulating extinction, poor relief, and lack of cleavage. In contrast to quartz crystals, the feldspar crystal contains impurities and only occasionally displays cleavage and increased relief. This sample thin section also contains a tiny number of biotite minerals with a brownish to dark brownish tint. Its pleochroism throughout the stage rotation is used to diagnose it. The detected minerals are found to have 45% k-feldspar, 45% quartz, 5% plagioclase, 5 % biotite as their modal percentages. The rock is identified as granite using a hand specimen, petrography, and geochemistry.

The main minerals in Sample D4S1G are feldspars, quartz, and a sizeable number of biotite crystals. The silicate minerals range in hue from pure white to colorless. Ondulous extinction is visible in these minerals as the microscope stage rotates. The range of grain sizes is ‘medium’ to ‘coarse’. This thin slice of rock contains 60% k-feldspar, 35% quartz, and 5% biotite as its modal mineral composition. Granite has been recognized as the rock.

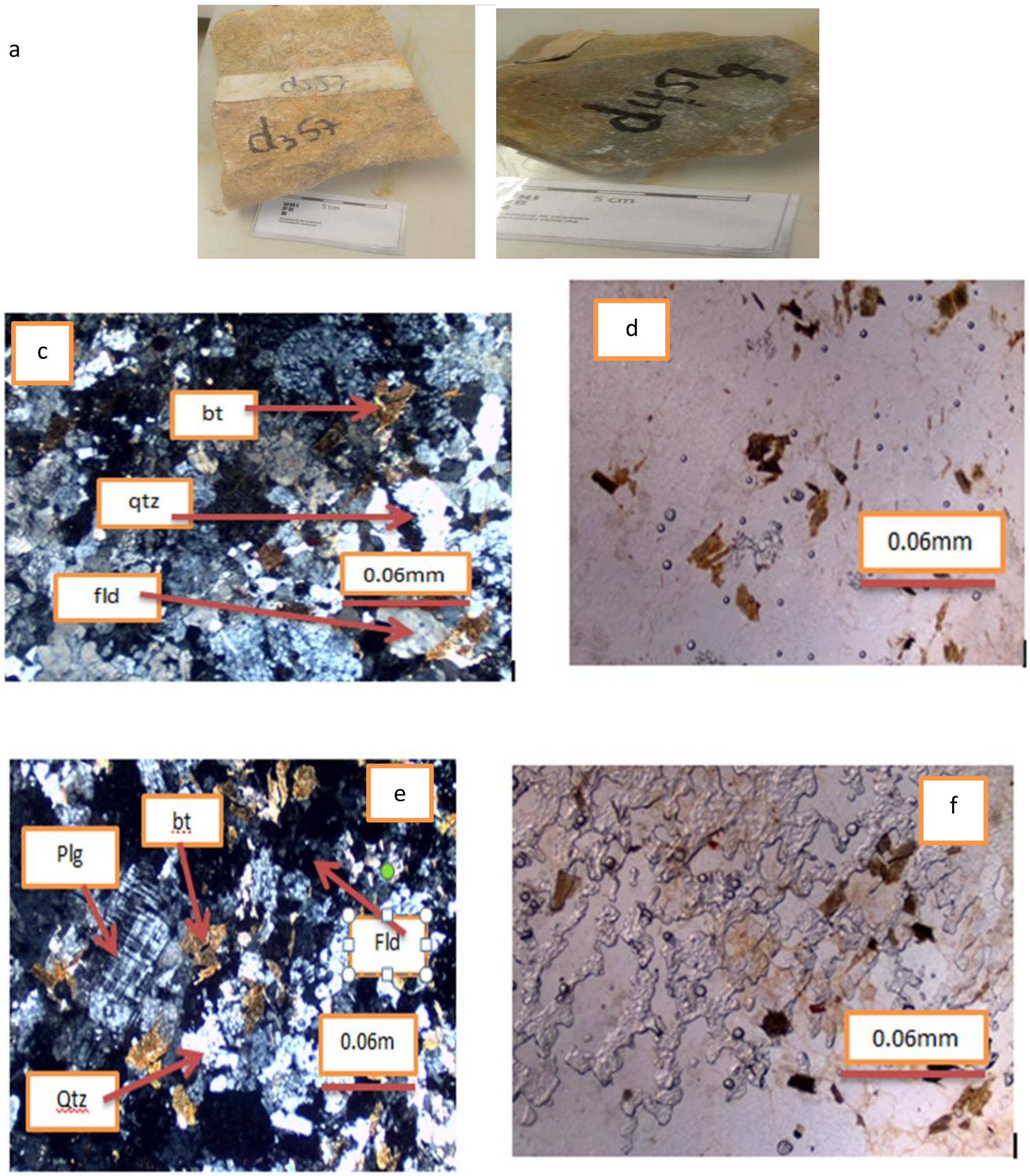

Figure 22: hand specimen and micro-photography of sample D3S7&D4S1G; a&b hand specimens; c&e XPL and d&f PPL views of thin section of D3S7& D4S1G respectively.

D4S1

Quartz, feldspar, plagioclase and biotite crystals make up Sample D4S1's structure. The crystals' grain sizes ‘range’ from ‘medium’ to coarse. On biotite minerals with brownish and somewhat greenish tones, cleavage is seen. The quartz crystals' surfaces have significant fractures. Hornblende minerals, with their dark, blue-greenish hues, are also occasionally found. About 30% k-feldspar, 10% clinopyroxene, 30% biotite, and 15% quartz. 10% plagioclase and 5% amphibole/hornblende are ‘found’ in the rock. According to a geochemical investigation, the rock is a diorite

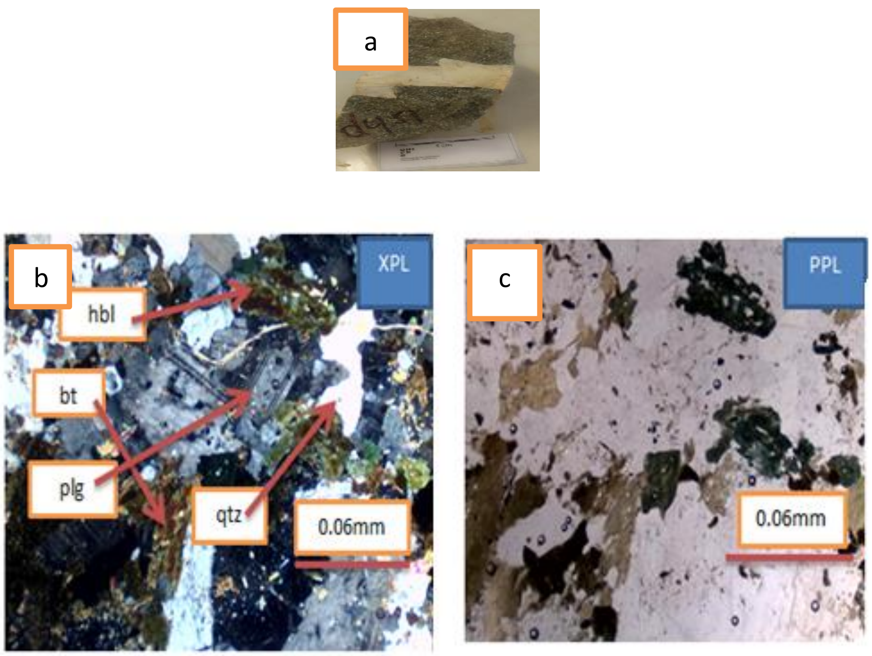

Figure 23: hand specimen and micro-photography of sample D4S1; a, hand specimen; b the XPL while c is the PPL views of the minerals seen in sample D4S1 thin section

Due to the amount of volcanic glass and other impurities present in some samples, it is typically only viable to classify the examined volcanic and granitoid rocks using their modal distributions, in samples with granular textures. Due to the estimates' imprecision and the rocks' extremely fine-grained texture, a geochemical categorization was chosen to give them names. The names that were provided here are therefore based on descriptions of hand specimens, petrography, and geochemical categorization (TAS classification).

CHAPER SIX

RESULTS AND INTERPRETATIONS

From the study area, 25 representative rock samples were taken. From these, two (D4S1G and D3S1) were chosen for petrographic examination only, two (D2S4 and D3S6) for geochemical analysis only, and seven samples (D1S-1, D2S-1 D2S-2, D2S-5) D3S-2 D3S-7' and D4S-1) were chosen for both petrographic and complete silicate geochemical analysis.

6.1 Petrography

The total of nine samples was sent to the Mekanissa branch of the institute of Geological Survey of Ethiopia for thin section preparation. The prepared thin section were then analyzed under the petrographic microscope in the Addis Ababa University school of earth science's petrographic lab and the results are shown as follows;

Table 6.1: petrographic results

Sample name	Observed minerals	Rock name
D2S1	Groundmass of fine plagioclase laths, rarely a phenocrysts of plagioclase crystals	Aphiric Basalt
D1S1	55% plagioclase, 40% olivine, 3% amphibole/hornblende, 1% pyroxene	Crystalline Basalt
D3S2	k-feldspar, quartz, and biotite are rarely seen in a glassy groundmasss	Rhyolite
D3S7	45% k-feldspar, 45% quartz, 5% plagioclase, 5 % biotite	Granite
D2S2	Groundmass of fine plagioclase laths, phenocrysts of altered olivine, and infilling quartz	Amygdaloidal basalt
D4S1	30% k-feldspar, 10% clinopyroxene, 25% biotite, 20% quartz. 10% plagioclase and 5% amphibole/hornblende	Diorite
D2S5	Mainly glassy but k-feldspar and Quartz crystals rarely seen	Rhyolite
D3S1	Olivine and plagioclase crystals in a ground mass of a very fine	Phyric Basalt

	grained plagioclase laths, opaque minerals and pyroxenes	
D4S1G	60% k-feldspar, 35% quartz, and 5% biotite	Granite

6.1.1 The QAP plot of granites

The QAP plot the classifies the granitic rock according to their concentration of Quartz, Alkali-feldaspar, plagioclase and feldspathoids put the granitic samples in the alkali-feldspar granite field. This is due to the fact that the granites in the study area are rich in alkali-feldspar followed by quartz.

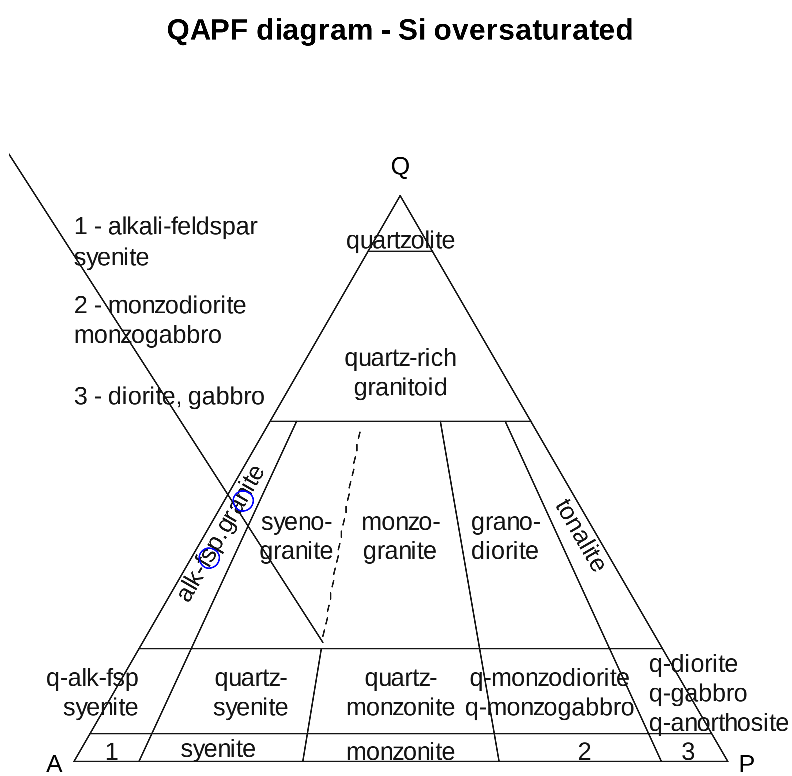

Figure 24: the QAP classification of Granites

6.2 Geochemistry

A total of nine (9) representative rock samples (D2S-4, D3S-2, D15-1, D2S-2, D3S-7, D4S-1, D3S-6, D2S-5, and D2S-1) were chosen for the examination of complete silicates (major oxides) in order to ascertain the 'geochemistry' of the 'rocks' in the research area. The concentration of major oxides is measured in percentages per sample. SiO_2, Al_2O_3, Fe_2O_3, CaO, MgO, NaO, K_2O, MnO, P_2O_5, TiO_2, and H_2O are among the main oxides identified. The classification and nomenclature of the rocks in 'the research area' are aided by the analysis of major oxides, which is also used to create the Harker diagrams that aid in comprehending the geochemical processes. The abundance and variable range with average (wt %) of several main oxides are shown in the accompanying table, which is the laboratory report for a thorough silicate geochemical examination of typical rock samples from the study area. samples were ground to a particle size of -200 mesh. Gravimetric, colorimetric, LiBO3, HF attack, and AAS methods were all applied. The certified geochemical reference materials (GRMs) were used to validate the analytical procedure, calibrate the instrument, and show the reliability and accuracy of the data. For each type of samples under analysis, GRMs with similar matrices and known elemental compositions were chosen. The same approach and instrument configuration were used to analyze the GRMs as they were for the studied samples. The accuracy was then evaluated by comparing the GRMS results to its known composition.

Table 6.2*: *Major Oxides in the Analyzed Samples as a Percentage

sample co	SiO2	TiO2	Al2O3	Fe2O3	MnO	MgO	CaO	Na2O	K2O	P2O5	H2O	LOI	Total
D2S-4	48.2	0.58	15.35	9.64	0.14	10.08	10.4	1.68	0.34	0.29	1.36	3.23	100.93
D3S-2	76.3	0.05	10.75	1.88	<0.01	0.04	0.32	4.14	3.62	0.1	0.47	1.23	98.91
D1S-1	49.48	0.38	16.97	8.66	0.08	9.32	10.52	1.9	0.42	0.16	0.99	2.62	101.5
D2S-2	44.26	1.02	15.79	8.64	0.12	6.6	10.54	1.48	0.46	0.36	3.93	6.18	99.38
D3S-7	74.6	0.08	15.79	1.02	<0.01	0.22	1.06	4.2	3.4	0.16	<0.01	0.55	101.1
D4S-1	59.62	0.54	16.64	6.52	0.12	2.62	8.02	3.72	1.7	0.68	<0.01	0.93	98.62
D3S-6	74.08	0.1	13.6	2.12	0.04	0.28	1.1	3.36	2.62	0.17	0.04	1.7	99.21
D2S-5	78.64	0.04	10.02	1.42	<0.01	0.36	0.44	2.52	3.22	0.16	1.59	2.28	100.7
D2S-1	48.34	0.7	18.59	9.6	0.16	6.74	8.1	2.72	0.62	0.36	1.07	2.29	99.19

The LOI for most samples lies between 0.55-3.23. One sample show a an LOI value of 6.18 which indicates its high Alteration.

In order to categorize rocks, major oxides are examined. Variation diagrams are then plotted, in which the chemical composition of the rocks is displayed alongside the outcome of experimentally collected data.

6.2.1 Classification of rocks in the research area Based on silica content

The rocks in the research area can be classified as felsic, intermediate, or mafic based on their silica (SiO**2**) content. The samples D2S-5 (78.64 w%SiO2), D3S-2 (76.30 w%SiO2), D3S-7 (74.60 w% SiO**2**), and D3S-6 (74.08 w%SiO_2) are categorized as felsic according to this categorization. Sample D1S-1 (49.48 w% SiO_2), Sample D2S-1 (48.34 w% SiO_2), Sample D2S-2 (44.2626 w% SiO_2), and Sample D2S-4 (48.20 w% SiO2) are mafic samples. Sample D4S-1 (59.62 w% SiO_2) is an intermediate sample.

6.2.2 The TAS classification of Rocks of the research area

The classification and nomenclature of the ‘rocks’ in ‘the research area’ is done using the TAS system. According to Hugh R. (1993) among the most helpful classification systems for volcanic rock is total alkali-silica. It was also used by Middlemost (1994) to classify plutonic rocks. Directly extracted from the rock analysis as w% oxides, the total alkali (TA), or combined total of Na_2O and K_2O contents, and the SiO_2 content are then plotted into the categorization diagram. Hugh R. (1993) states that Cox et al. (1979), who proved that there are reliable theoretical justifications for selecting SiO2 and Na_2O + K_2O as a basis for categorization, demonstrated the usefulness of the TAS diagram. Since both volcanic and plutonic rocks make up the study area samples, the TAS diagram is drawn appropriately to show the precise classification and naming of the ‘rocks’ of ‘the study area’ according to their total alkali versus silica concentrations.

...i Classification of plutonic rocks in the research area

Three representative samples of plutonic rocks from the study area's plutonic rocks were sent to the geological institute of Ethiopia's geochemistry lab for a full silicate geochemical analysis. Accordingly, two of the samples are classified as ‘belonging’ to the granitic field based on their total alkali versus silica (TAS) contents, whereas one sample is classified as a diorite (fig 29). The diorite unit which was found in the research region along a road cut close to Mountain Biibo, a short distance from the area's significant granitic exposure. The rhyolite exposure of the Undu Mountain ridges coexists with the granitic unit.

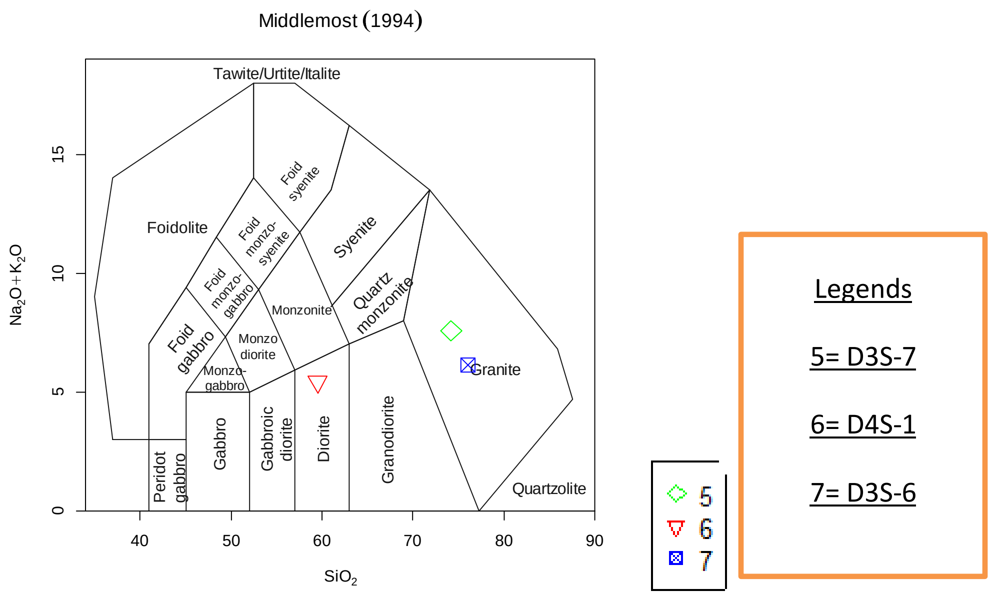

Figure 25: TAS classification of the plutonic samples from the study area; middlemost (1994).

...ii Classification of volcanic rocks of the research area

For a geochemical investigation, six representative volcanic rock samples were chosen. Four of the samples are classified as basaltic in the TAS clasification based on their total alkali versus silica concentration, while the other two are classified as rhyolite (Fig 30).

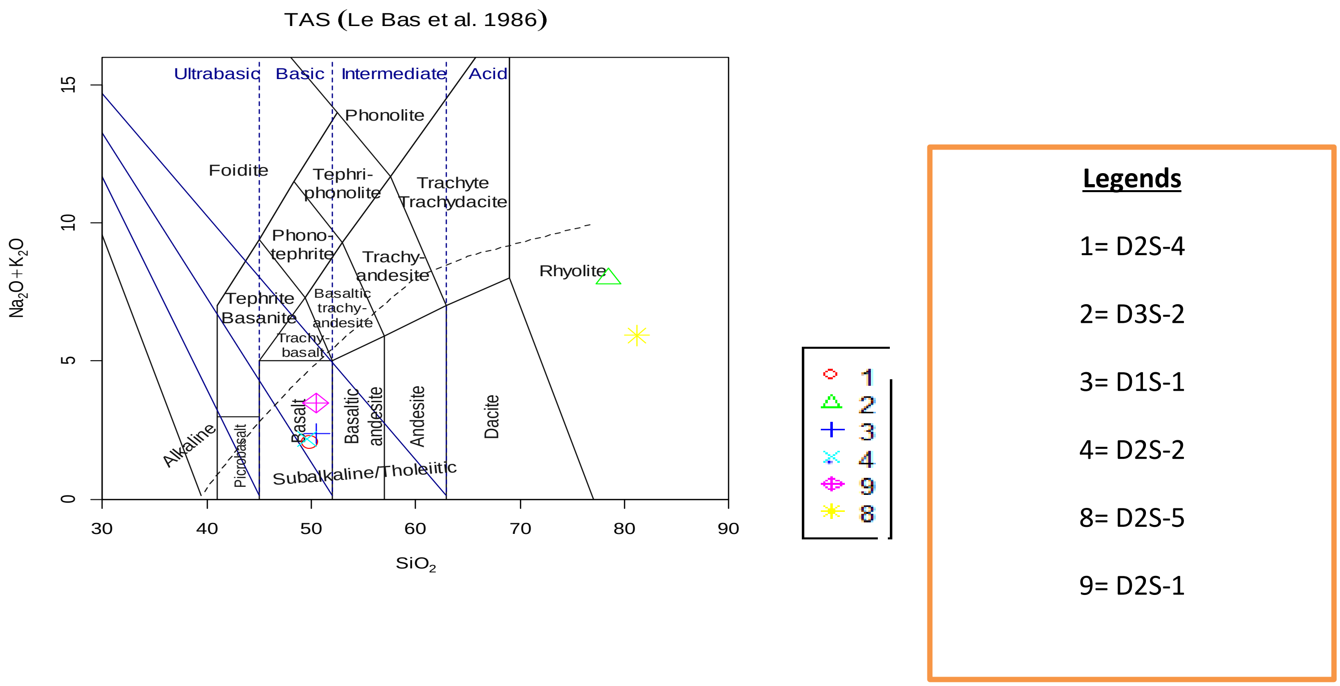

Figure 26: TAS classification of the meta-volcanic rock samples from the study area after Le Bas et al. (1986)

Plots of major oxides vs silica

The main oxides exhibit a variety of values according to the laboratory study. Silica (SiO_2) (44.2–78.64), alumina (Al_2O_3) (10.–21.59), ferric oxide (Fe_2O_3) (1.02–9.54), lime (CaO) (0.3–10.54), magnesium (MgO) (0.04–10.08), soda (Na_2O) (1.48–4.20), potash (K_2O) (0.34–3.62), manganese (MnO) (<0.01-0.16), phosphorus (P_2O_5) (0.10-0.68), Titania (TiO_2) (0.04-0.70), and water (H_2O) (<0.01-3.93) (table 6.1). Because the plutonic rocks in the study area are much older than the volcanics, they are ploted separately. For the granitic samples of the research area, TiO_2 Al_2O_3 MgO CaO P_2O_5 and FeOt show a negative trend with the rising concentration of SiO2 w% in the major oxides vs. silica diagram (Harker diagram). Granitic rocks are most likely the consequence of fractional crystallization during magmatic evolution, supported by the separation of apatite and mafic minerals during crystallization, according to the overall major elements on the Harker diagram plot that show negative trend correlation with regard to SiO_2. According to Adi et al. (2012), as stated in Natnael, w. (2018), the decline in the concentration of TiO_2 and P_2O_5 with the increase in SiO_2 concentration is an ‘indication’ of the fractionation of minerals such as apatite and ilmenite. As SiO_2 concentration increases due to fractional crystallization,

Al_2O_3 exhibits a random negative trend, according to Natnael, W. (2018), Al_2O_3 versus SiO_2 exhibits two patterns, one of which is upward to the curve denotes the absence of crystallization, but the inflection that occurs beyond the curve denotes the presence of crystallization sequences. The greater concentration of Al_2O_3 in the granitoid rocks of ‘the research area’ suggests that minerals like plagioclase, amphibole, and biotite have helped to enrich the rock samples (Natnael, 2018). The trends for Na_2O and K_2O are scattered with the increase in SiO_2 w% concentration. The scattered trend of K_2O and Na_2O versus silica suggests that there has been only minor alteration of feldspars and plagioclases, or that the granite rocks are rich in alkali feldspar and biotite, or that there has been contamination of the magma that formed the rocks, as stated in Natnael Wondera (2018). The ‘basaltic’ and ‘rhyolitic’ rocks of the study area's main oxide against silica plot exhibit the same pattern as the granitic rocks. Plots of the major element oxides against SiO_2 showed that the concentrations of TiO_2 Al_2O_3 MgO CaO P_2O_5 and FeOt decreased with the concentration of SiO_2 (fig 27&28; a, b, c, d, g and h respectively), while the concentrations of Na_2O and K_2O increased (fig, 27&28 e&f). This pattern matches Bowen's hypothesized pattern for basaltic magma crystallization (Roland et al., 2020). According to Hughes R. (1993), the inflection in the plots of ‘major oxides’ on the TAS diagram typically denotes either the entry of a new phase during crystal fractionation or the loss of an existing phase during partial melting. As can be seen under a petrographic microscope in thin sections of these samples from ‘the research area’, this may suggest that the rock ‘units’ in ‘the research area’ were created by fractoinal crystallization and that the abundance of minerals like plagioclase and biotite in their composition. With the increases in SiO_2, CaO and MgO levels are falling as well. Plagioclase and clinopyroxene's coprecipitation of these oxides from the liquid is indicated by the CaO demonstrating positive corelation with Mg.

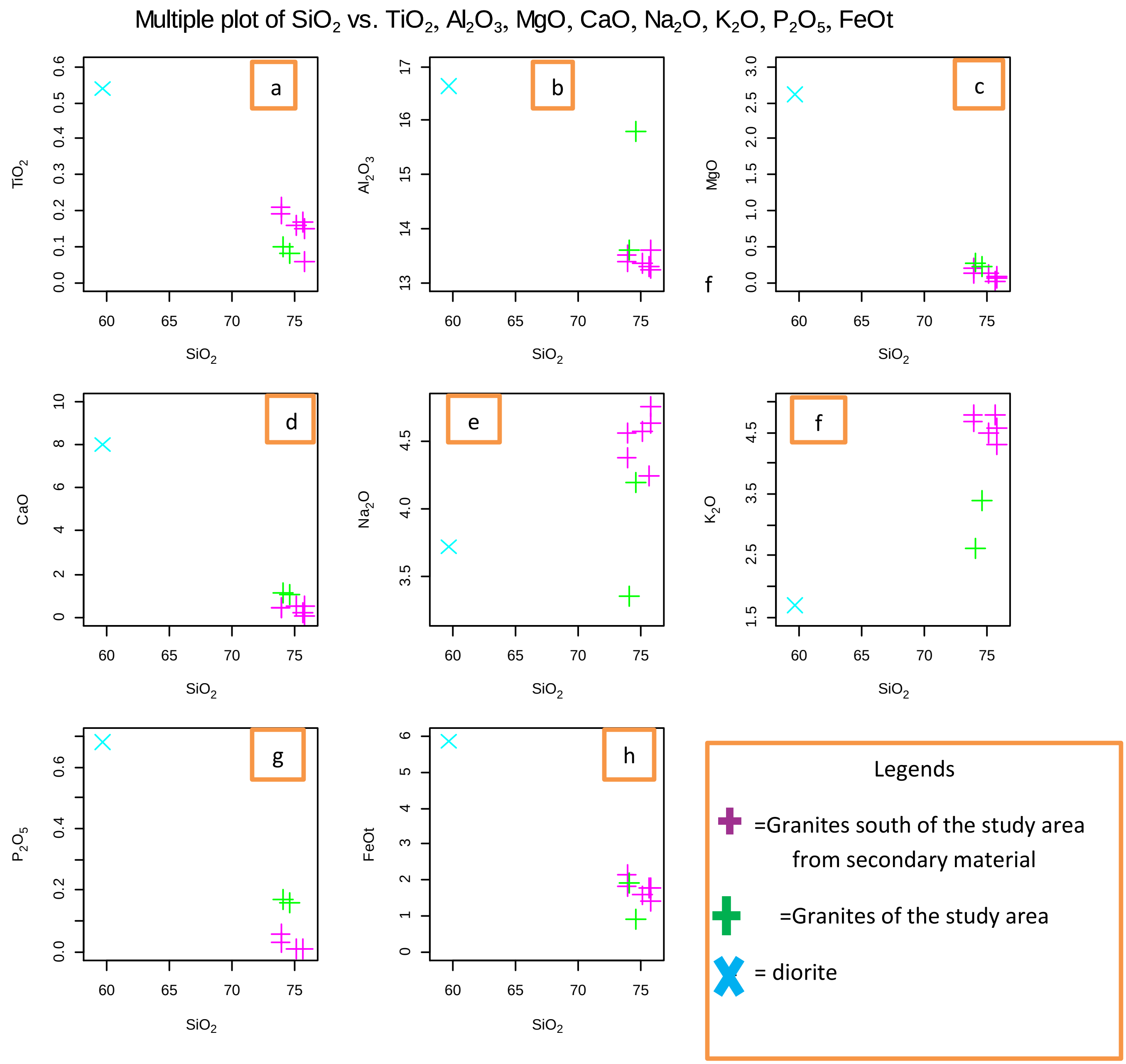

Figure 27: plots of major oxide vs silica content of plutonic 'samples' from the research area, and south of the study area from the work of Natnael Wondera (2018); a TiO_2 vs SiO_2, b Al_2O_3 vs SiO_2, c MgO vs SiO_2, d CaO vs SiO_2, e Na_2O vs SiO_2, f K_2O vs SiO_2, g P_2O_5 vs SiO_2, h FeO(t) vs SiO_2.

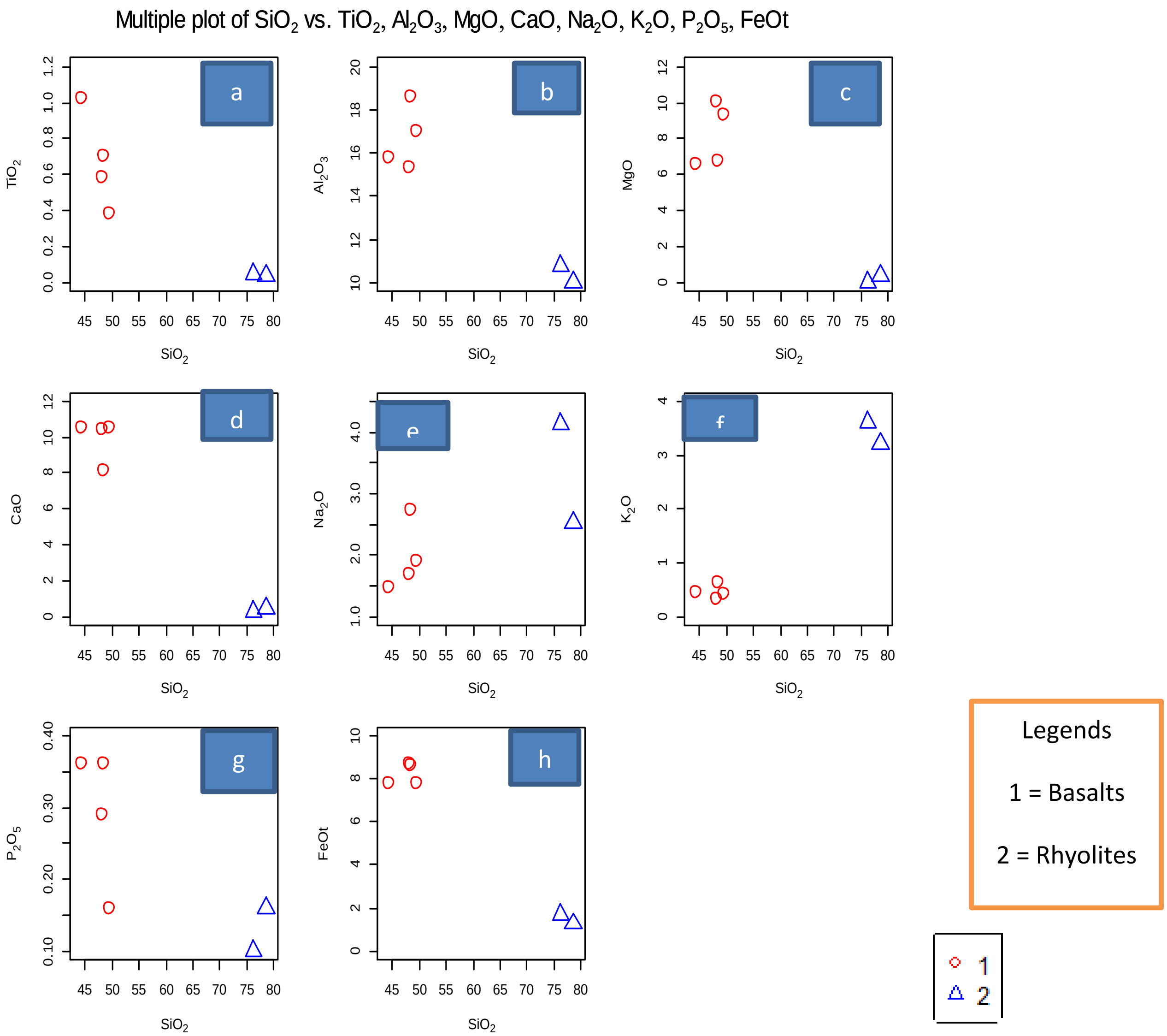

Figure 28: major oxides vs silica plot of volcanic samples

6.3 AFM classification

The research area's felsic rocks, including the granitic rocks and rhyolites, are classified by AFM as belonging to the calc-alkaline series, whereas the basaltic samples are classified as belonging to the tholeeitic series. The basaltic rocks are placed in the right corner of the tholeetic field that indicates the high content of iron. AFM is a ternary diagram that illustrates the relative abundances of alkali, iron, and magnesium oxides in igneous rocks. The diagram's elements are therefore A (Alkalis: Na_2O + K_2O), F (FeO & Fe_2O_3), and M (MgO) (https://observablehq.com/@julesblm/afm-diagram-of-igneous-petrology).

Though not always reliable due to contamination or alteration, the rocks placed in the calk-alkaline field of the AFM diagram are related to continental arcs (Emily J. Chin et al., 2018). So the AFM diagram of the samples of the study area show that granites, diorite, and rhyolites are of continental arc. The basalts are placed at the inclination of the tholeetic line to the right that indicates they are of transitional type and are associated to the subduction zone or back arc basin

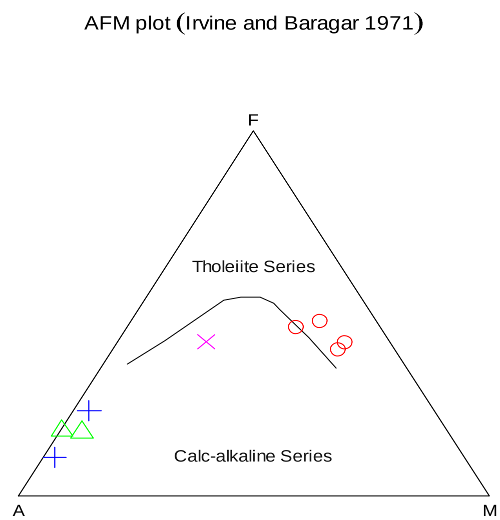

Figure 29: AFM plot of representative rock samples of the 'research area' after Irvin and Bargar (1971)

CHAPTER SEVEN

DISCUSSIONS AND SUMMARY

7.1 Introduction

this study was carried out to identify the lithological units of 'the research area' in terms of their petrographic description and geochemical composition, to know their classification and nomenclature, to identify the grade of metamorphism that gave rise to them, and to determine the temperature and pressure conditions that led to their formation. It also aimed to produce a lithological map that depicted their distribution within the study area. In order to achieve this goal, fieldwork was done to investigate how different rock types were exposed. Representative rock samples were then brought, which were then used for geochemical 'analyses as well as petrographic investigation.

7.2 Geology of the study area

The wide majority of 'the research area' is determined to be covered by the granitoid exposure during fieldwork. Additionally, basaltic rocks are seen in Mountain Dul Undu, which is close to the Fametsere village in the Kurmuk district, and in the flat areas close to Homosha (Komosha) town. In a minor exposure close to the granitic rock exposure along the Assosa-Homosha road near Mountain Bibo, one rock sample that was identified as diorite was discovered. According to Mengesha (1991), granitic rocks found in the research area are severely deformed and recrystallized. The 652 million year age of the Komosha syntectonic granite, which falls within the late Proterozoic, may denote a metamorphic phase, according to Menegesha (1991).

Near Bamadhon hamlet, felsic rock known as rhyolite was discovered on top of weathered basalt. It also forms the two ridges of Mount Undu. The wide majority of 'the research area' is determined to be covered by the granitoid exposure during fieldwork. Additionally, basaltic rocks are seen in Mountain Dul Undu, which is close to the Fametsere village in the Kurmuk district, and in the flat areas close to Homosha (Komosha) town. In a minor exposure close to the granitic rock exposure along the Assosa-Homosha road near Mountain Bibo, one rock sample that was identified as diorite was discovered. Near Bamadhon hamlet, felsic rock known as rhyolite was discovered on top of weathered

basalt. It also forms the two ridges of Mount Undu. According to Mengesha Tefera (1991), the granitic mass (Komosha granite) north of Asosa has an uneven shape but foliation that runs north to south. In his work, Mengesha Teferra described the Undu Mountain as a granite and volcanic massif; this investigation discovered that two of the Undo Mountain's ridges and the neighboring hills are rhyolites. The petrography, geochemical studies, with a 'description' of the hand specimens from the rocks all supports this. In the studied area, flat areas between the isolated granite hills are occupied by basalts. According to Mengesha Tefera (1991), basalt flows only cover a minor portion of 'the research area'. He claims that the Tertiary volcanic rocks that once covered most of the 'area' is now only found as residual capping. He stated that while there are currently no isotopic dates available, it is believed that these basalts are Tertiary in age and that 'most' of the flows are fissural in nature. He added that these occurrences resemble extensions of the central Ethiopian plateau's Tertiary volcanics and the Tertiary volcanics found south of 'the research area'.

7.3 Petrography

According to this study's petrographic description, the granitoid rock contains the minerals feldspars, quartz, biotite, hornblende, and opaque. Plagioclase, olivine, pyroxenes, biotite, hornblende, and opaque minerals are all found in basalts. It was discovered that the rhyolite samples contained feldspars. Menegesha Tefera (1991) further mentions that 'thin sections reveal' the rock in 'the research area' to be a coarse-grained, igneous-textured leucogranite. The main minerals are quartz, albite/oligoclase, and microcline; the auxiliary minerals include biotite, hornblende, opaques, muscovite, sphene, and zircon. There is Perthite. According to him, sericite, epidote, and chlorite are altered in feldspars and biotite. Quartz exhibits a wavy extinction pattern. Plagioclase, olivine, pyroxenes, biotite, hornblende, and opaque minerals have all been found in the basalts examined during this study. According to Mengesha Tefera (1991), the study area's basalt has undergone extensive weathering and is covered in a lateritic crust. There are basalt flows that are aphyric and porphyritic with olivine or pyroxene phenocrysts. The aphyric basalt is fine-grained and has a holocrystalline, pilotaxitic groundmass of elongate plagioclase laths, augite, and copious olivine, some of which forms clustered microphenocrysts, according to thin sections of the rock. He proposed that the predominant minerals are labradorite (35–40%), olivine (20–25%), augite (20–25%), and magnetite (10–15%). Phlogopite, apatite, haematite, and chlorite are the minor minerals. He came to the 'conclusion' that the porphyritic basalt had a pilotaxitic groundmass formed of plagioclase microlites, pyroxene, olivine, and magnetite, and had an ophitic texture with massive phenocrysts of clinopyroxene and olivine. According to this study's petrographic description, the granitoid rock contains the minerals feldspars, quartz, biotite, hornblende, and opaque. Plagioclase, olivine, pyroxenes, biotite, hornblende, and opaque minerals are all found in basalts. It was discovered that the rhyolite samples contained feldspars, quartz, and biotite.

7.4 Geochemistry and fractional crystallization

The major oxides that were examined in the rock samples for major element geochemistry have varying contents. According to the results, the major oxide concentrations were 44.26-78.64w% SiO_2, 10.2-18.59w% Al_2O_3, 1.02-9.64w% Fe_2O_3, 0.32-10.54w% CaO, 0.04-10.08w% MgO, 0.34-3.62w% K2O., <0.01-0.16w% MnO, 0.10-0.68w% P_2O_5, 0.04-1.02w% TiO_2 and <0.01-3.93w% H_2O (table 6.1). Samples D2S-5, D3S-2, D3S-7, and D3S-6 are felsic in terms of their SiO_2 content (78.64, 76.30, 74.60, and 74.08 w%SiO_2, respectively). While samples D1S-1 (49.48 w%SiO_2), D2s-1 (48.34 w%SiO_2), D2S-2 (44.2626 w%SiO_2), and D2S-4 (48.20 w%SiO_2) are mafic in type, and D4S-1 (59.62 w%SiO_2) is intermediate. This relates to the Asosa terrain's Dul domain, according to Tadesse Alemu's 2007 classification. The Dul domain is characterized by several different lithological units, such as volcanic and sedimentary successions metamorphosed to the 'greenschist facies', associated with mafic-ultramafic rocks, and 'granitoid intrusives' (Ahmed 1982; Abnet 1989; Negussie 1988; Wollie Sheka et al. 1990; Mersha et al. 1995; Bekele 1999; Guliev 1982; Soukhoroukov (1980).

Two samples (D3S-6 and D3S-7) are categorized as granite when categorized using TAS, one sample (D4S-1) is classified as diorite, two samples (D3S-2 and D2S-5) are classified as rhyolites, and four samples (D1S-1, D2S-1, D2S-2, and D2S-4) are classified as basalts. TiO_2, Al_2O_3, MgO, CaO, P_2O_5 and FeOt concentrations decreased with increasing SiO_2 concentration in multiple plots of SiO2 versus major oxides (fig 30&31 a, b, c, d, g&h), However Na_2O and K_2O concentrations increased. Fractional crystallization is supported by this evidence. According to Mengesha Tefera (1991), the low initial 87Sr/86Sr ratio of 0.70811 for the granite in 'the research area' points to a mantle-derived magma that underwent fractional crystallization with little contamination by previous crustal rocks. The mafic rocks in 'the research area' are classified as tholeiitic, whilst the felsic rocks are classified as belonging to the calc-alkaline series by the AFM.

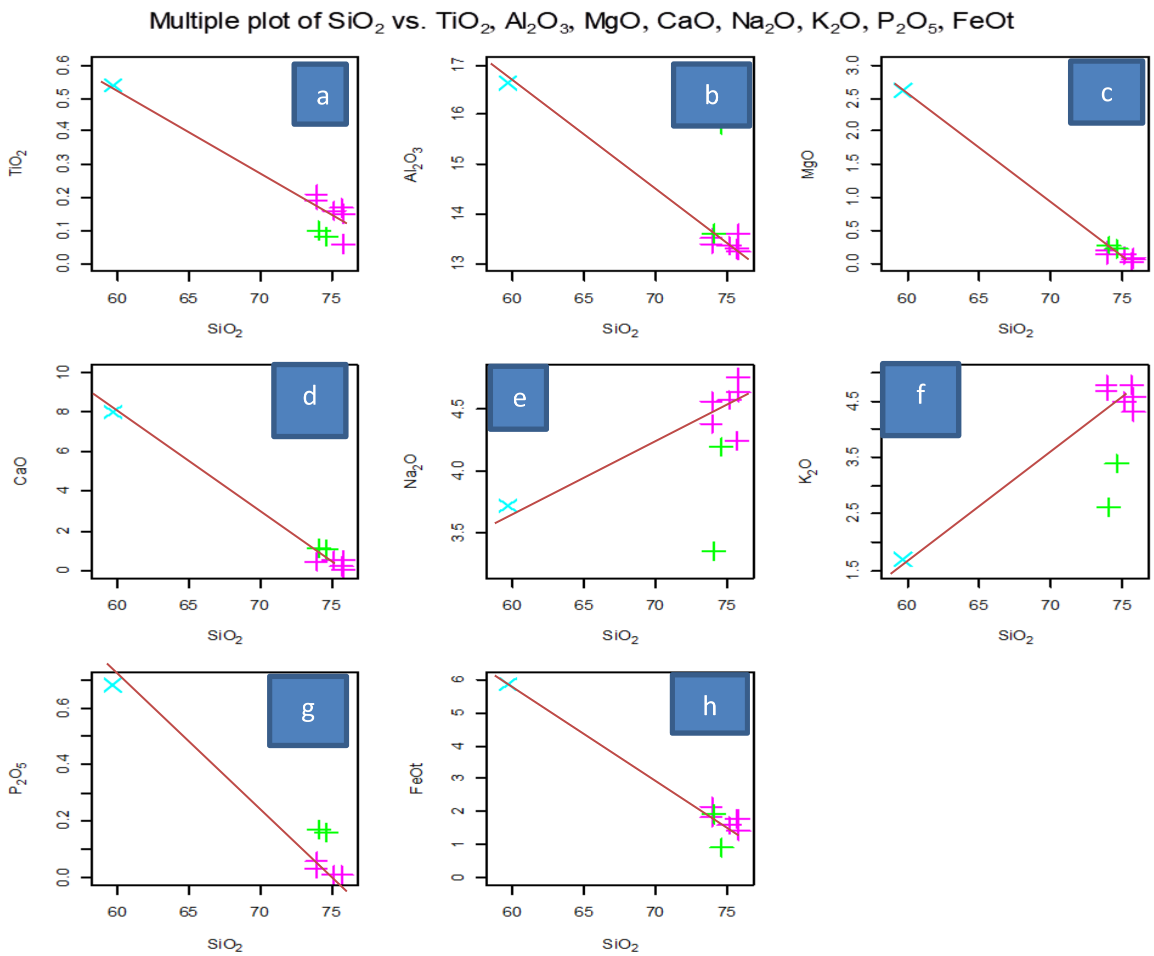

Figure 30: plots of major oxides vs silica of plutonic samples; a, TiO_2 vs SiO_2; b Al_2O_3 vs SiO_2; c, MgO vs SiO_2; d, CaO vs SiO_2, e, Na_2O vs SiO_2; f, K_2O vs SiO_2; g, P_2O_5 vs SiO_2, and h, FeOt vs SiO_2

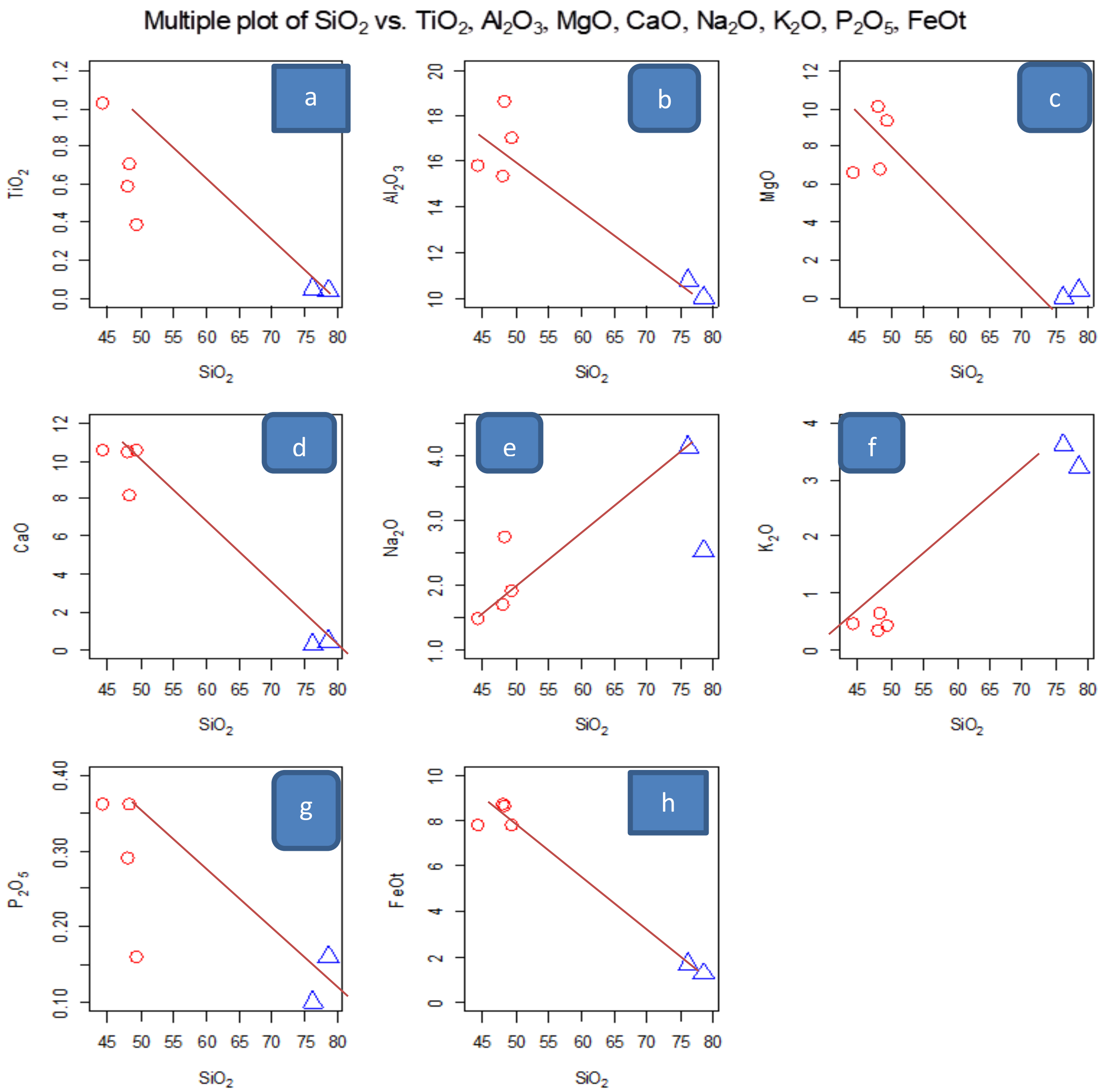

Figure 31: Major oxides vs SiO_2 plot of volcanic samples; a, TiO_2 vs SiO_2; b Al_2O_3 vs SiO_2; c, MgO vs SiO_2; d, CaO vs SiO_2, e, Na_2O vs SiO_2; f, K_2O vs SiO_2; g, P_2O_5 vs SiO_2, and h, FeOt vs SiO_2

7.5 Geotectonic settings

A, granitoids

According to the Sylvester diagram, the granitoid rocks in the research area have a peraluminus affinity while the granites south of the study area have alkaline affinity. A Sylvester diagram shows the major elements that make up granitic rocks graphically. FeO/FeO+MgO), the modified alkali-lime index (MALI), and the aluminum saturation index (ASI) serve as its foundation. Based on their geochemical properties, granitic rocks are divided into several groups using the diagram. This indicates that the granitoid of the study area and neighboring southern Assosa granite are of mantle and crustal origion respectively

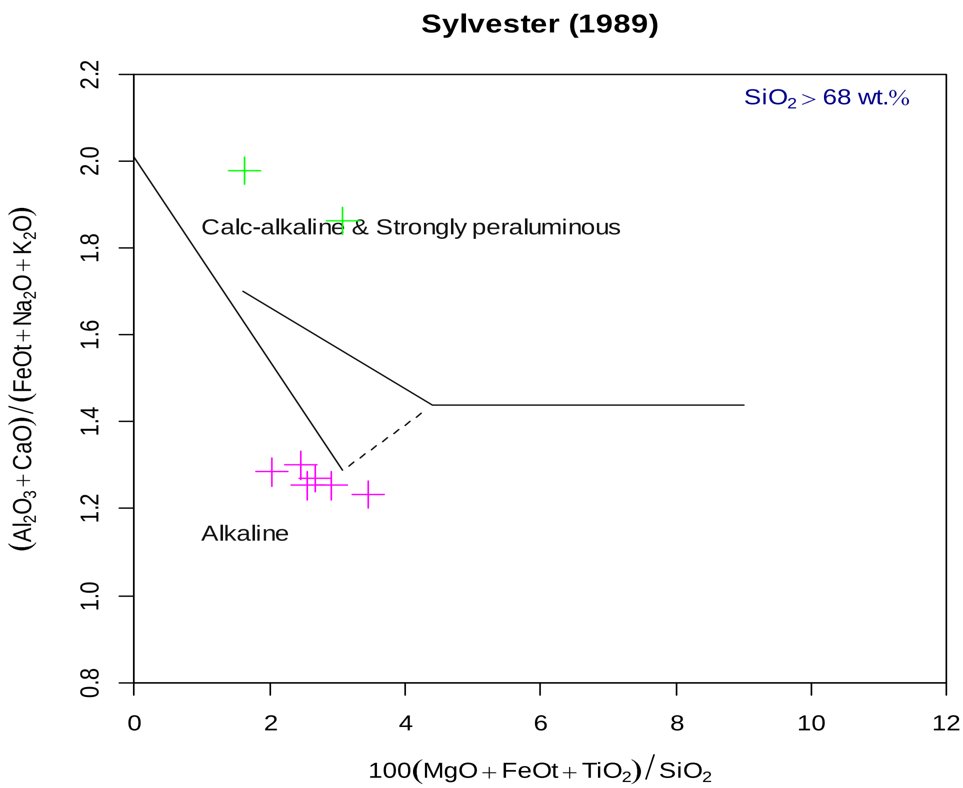

Figure 32: the sylvester diagram of granitic rocks after Sylvester (1989)

The R1-R2 diagram of Batchelor and Bowden (1985) shows that, the granitic exposures in the study area and its surroundings are related to syn-collision. Diorite is related to pre-plate collision.

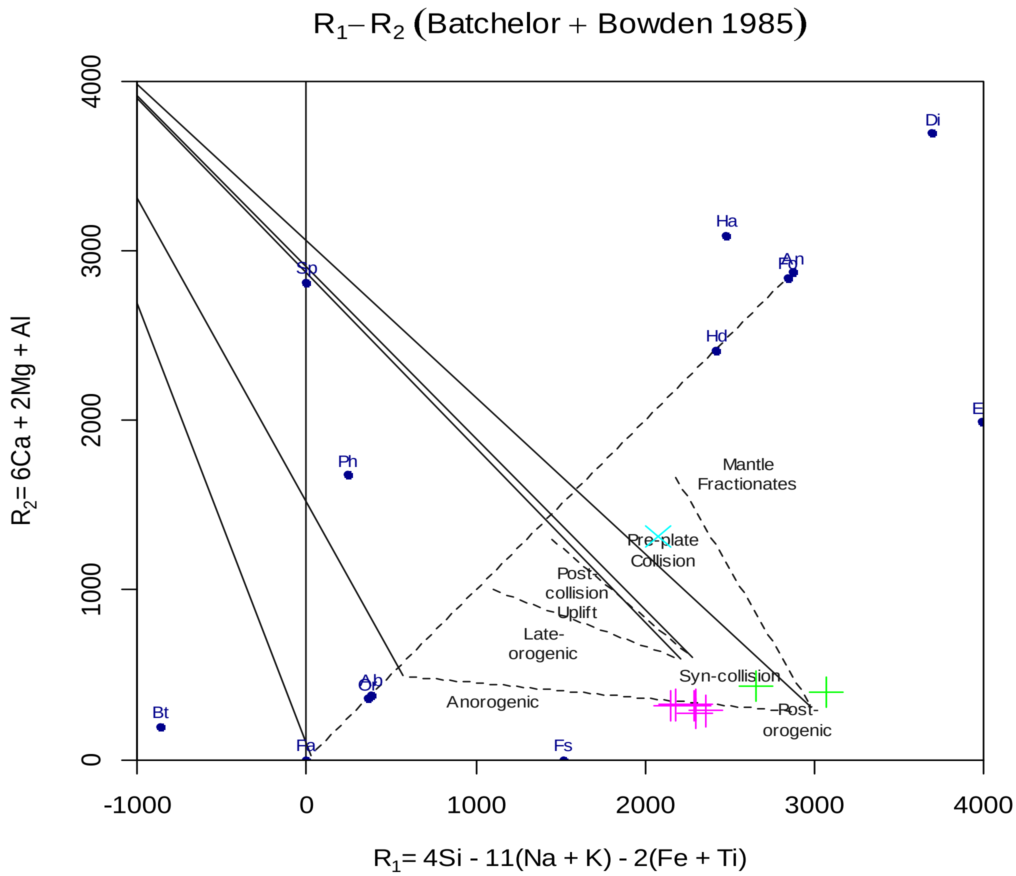

Figure 33: the R1-R2 diagram of granitic rocks after Batchelor and Bowden (1985)

B) Basalts

Ploted on the 10MnO-TiO2-10P2O5 diagram of Mullen (1983), all the samples fall in the calc-alkaline Basalt (CAB) field. This indicates that they are formed along subduction zones or continental arcs

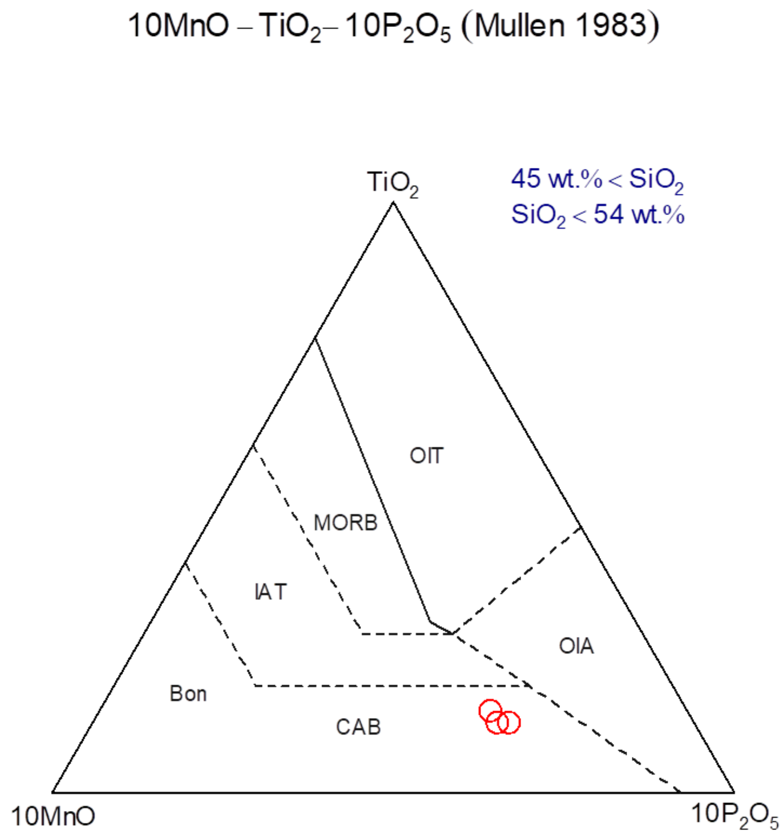

Figure 34: the 10MnO-TiO2-10P2O5 diagram of Basaltoids after mullen (1983)

CHAPTER EIGHT

CONCLUSIONS AND RECOMMENDATIONS

8.1 Conclusions

We came at the following conclusions based on field descriptions, petrographic analysis, and interpretations of geochemical and petrographic data:

1. ‘The research area’ is shielded from lithological units with compositions ranging from mafic to felsic. Meta-granites, meta-rhyolites, meta-basalts, and meta-diorites are some of these components. Much of the land is covered in meta-granite.
2. The major oxide against silica (SiO_2) plots showed that the basaltic magma fractionally crystallized to create the rocks in the research area, which were then contaminated by crustal elements. This is demonstrated by the fact that when SiO_2 concentrations grew, the concentrations of Na_2O and K_2O increased, while TiO_2, Al_2O_3, MgO, CaO, P_2O_5 and FeOt concentrations decreased. Also supporting fractional crystallization in ‘the research area’ is the occurrence of intermediate meta-diorite.

Recommendations

- This study represents a tiny percentage of the area, so I suggest creating a large-scale map of the 'area' that stretches to the Ethiopian-Sudanese border so that greater work may be done to reflect the entire area.
- In order to understand more about the studied area, I advise conducting trace element, isotopic, and rare earth element analysis. This study was only conducted using a petrographic study and the major oxide geochemical analysis.
- Numerous economically significant minerals can be found in 'the research area'. Locals and small-scale businesses are only engaged in gold extraction, so I advise further research be done on the other mineral resources to see where they are concentrated and how important they are economically.

References

Abdelsalam, M., Tsige, L., Yihunie, T., and Hussien, B. (2008). Terrane rotation during the East African Orogeny: evidence from the Bulbul Shear Zone, south Ethiopia. Gondwana Res., 14(3), 497–508.

Abdelsalam, M.G. and Stern, R.J. (1996). Sutures and shear zones in Arabian-Nubian Shield. *Journal of African Earth Sciences*, 23(3), 289–310.

Abnet, Z. (1989). Gold Mineralization at Dul, Kurmuk District, Asosa Administrative Region. Ethiopian Institute of Geological Surveys, technical report 900-351-01, p 18

Abraham, A. (1989). Tectonic history of the pan-african low-grade belt of western ethiopia. Ethiopian Inst Geol Surv Note No. 305, p 14

Abraham, A., (1989). Tectonic history of the Pan-African low grade belt of western Ethiopia. Eth. Inst. Geol. Surv., Note No. 305 p. 15.

Adi, Maulana, Koichiro, Watanabe, Akira, Imai, Kotaro, and Yonezu (2012). Petrology and Geochemistry of Granitic Rocks in South Sulawesi, Indonesia: Implication for Origin of Magma and Geodynamic Setting. International journal of Environmental, Chemical, Geological and geophysical Engineering. 6:1

Ahmed, M. (1982). Report on Kurmuk-Gizen Integrated Mineral Exploration Project. Ethiopian Inst Geol Surv Note No. 208

Alemu T., Abebe, T. (2007). Geology and tectonic evolution of The Pan-African Tulu Dimtu Belt, western Ethiopia. *Medwell Online J Earth Sci,* 1, 24–42

Alemu, T., and Abebe, T. (2000). Geology of the Gimbi area. Geol Surv Ethiopia, Memoir 15, p156

Allen, A,. and Gebremedhin Tadesse (2005). Reply to Discussion of ‘‘Geological setting and tectonic subdivision of the Neoproterozoic Orogenic Belt of Tuludimtu, Western Ethiopia’’. *Journal of African Earth Sciences*, 41, 333–336.

Allen, A., and Gebremedhin Tadesse (2003). Geological setting and tectonic subdivision of the Neoproterozoic orogenic belt of Tuludimtu, Western Ethiopia. *Journal of African Earth Sciences,* 36, 329–343.

Almond, D.C., (1983). The concept of Pan-African Episode and Mozambique Belt in relation to the geology of east and northeast Africa. Bulletin of the Faculty of Earth Sciences, King Abdulaziz University Jeddah, 6, 71–88.

Andreoli, M.A., (1981). The amphibolite and the granulite facies rocks of southern Malawi. PhD Thesis, University of Witwatersrand, S. Africa, 351 pp.

Avigad, D., Stern, R.J., Beyth, M., Miller, N., and Mc Williams, M.O. (2007). Detrital zircon UPb geochronology of Cryogenian diamictites and Lower Paleozoic sandstone in Ethiopia (Tigrai). age constraints on Neoproterozoic glaciation and crustal evolution of thesouthern Arabian Nubian Shield. Precambrian Research, 154, 88–106.

Ayalew, T. (1997). Metamorphic and Structural Evolution of the Gore-Gambela Area, Western Ethiopia. SINET: *Ethiopian Journal of Science*, 20(2). https://doi.org/10.4314/sinet.v20i2.18103.

Ayalew, T., and Johnson, T. (2002). The geotectonic evolution of the Western Ethiopian Shield. *Ethiopian J. Sc*., 25 (2), 227–252.

Ayalew, T., Bell, K., Moore, JM., and Parrish, RR. (1990). U–pb and Rb-sr geochronology of the western Ethiopian shield. *Geol Soc Am Bull* 102, 1309–1316B

Ayalew, T., Bell, K., Moore, JM., and Parrish, RR. (1990). U–pb and Rb-sr geochronology of the western Ethiopian shield. Geol Soc Am Bull, 102, 1309–1316

Bekele, M. (1999). Geological and geochemical conditions for the occurrence of gold in Dul area, western Ethiopia. PhD. Dissertation, Institute of Petrology, University of Vienna, p 209

Berhe, S.M. (1990). Ophiolites in Northeast and East Africa: implications for Proterozoic crustal growth. *Journal Geological Society of London*, 147, 41–57.

Berhe, SM. (1990). Ophiolites in northeast and east Africa: implication for Proterozoic crustal growth. *J Geol Soc London* 147, 41–57

Bingen, B., Viola, J., Henderson, I., Skar, O., Boyd, R., Thomas, R., Solli, A., Key, R., and Daudi, E. (2009). Geochronology of the Precambrian crust in the Mozambique belt in NE Mozambique and implications for Gondwana assembly. Precambr. Res., 170, 231–255.

Blades, M. (2013). Age and Origin of the Western Ethiopia Shield. University of Adelaide.

Blades, M.L., Collins, A.S., Foden, J., Payne, J.L., Xu, X., Tadesse Alemu, Girma Woldetinsae, Clark, C., and Taylor, R.J.M. (2015). Age and Hafnium isotopic evolution of the Didessa and Kemashi Domains, western Ethiopia. Precambrian Research, 270, 267–284

Bonavia, F., and Chorowicz, J. (1992). Northward expulsion of the Pan-African of northeast Africa guided by a reentrant zone of the Tanzania craton. *Geology* 20, 1023–1026.

Braathen, A., Grenne, T., Selassie, M.G., and Worku, T. (2001). Juxtaposition of Neoproterozoic units along the Baruda-Tulu Dimtu shear belt in the East African Orogen of western Ethiopia. Precambrian Research, 107, 215–234.

Britannica, The Editors of Encyclopaedia. "greenschist facies". Encyclopedia Britannica, 8 Dec. 2006, https://www.britannica.com/science/greenschist-facies. Accessed 16 May 2023.

Caen-Vachette, M. (1977). Geochronologie du Precambrien Malgache. *Bulletin de lAcademie Malgache*, 55, 251–289.

Caen-Vachette, M. (1979). Le Precambrien de Madagascar. Radiochronometrie par isochones Rb/Sr sur roches totales. *Revue de Geologique dynamique et Geographie physique*, 21, 331–338.

Cahen, L., Snelling, N.J., Delhal, J., Vail, J.R., Bonhomme, M., and Ledent, D. (1984). The Geochronology and Evolution of Africa. *Clarendon Press*, Oxford. 512 pp.

Chappell, B.W., and White, A.J.R. (1974). Two contrasting granite types. *Pac. Geol.*, 8, 173–174.

Chater, A.M. (1971). The Geology of the Megado Region of Southern Ethiopia. PhD Thesis, University of Leeds, UK, 343 pp

Chen, T. (20010. The Mozambique Belt: the link between East and west Gondwana in the Neoproterozoic and possible connection with the Trans-Antarctic Mountains. *Gondwana Res.*, 4, 594–595.

Clark, C., and Taylor, R.J.M. (2015). Age and Hafnium isotopic evolution of the Didessa and Kemashi Domain, western Ethiopia. *Precambrian Research*, 270, 267-284.

Costa, M., Ferrara, G., Saachi, R., and Tonarini, S. (1992). Rb/Sr dating of the upper Proterozoic basement of Zambezia, Mozambique. *Geologische Rundschau*, 81, 487–500.

Davidson, A. (1983). The Omo river project: reconnaissance geology and geochemistry of parts of Illubabor, Kefa, Gamu Gofa and Sidamo, Ethiopia. Ethiopian Inst Geol Surv Bulletin 2:89

De Waele, B., Kampunzu, A., Mapani, B., and Tembo, F. (2006). The Mesoproterozoic Irumide belt of Zambia. *J. Afr. Earth Sc.*, 46, 36–70.

de Wit MJ., and Aguma, A. (1977). Geology of the ultramafic and associated rocks of Tullu Dimtu, Wollega. Ethiopian Inst Geol Surv 57:28

De Wit, M.J., Berg, R., Balcha, B., Guyasa, A., and Bekele, T.(1977). Geology of the Kata area,Welega. Unpublished Report, 65, Ethiopian Institute of Geological Surveys,14p.

De Wit, M.J., and Abera Aguma (1977). Geology of the ultramafic and associated rocks of Tullu- Dimtu,Welega. Unpublished Report, 57, Ethiopian Institute of Geological Surveys, 23pp.

de Wit, M.J., and Senbeto Chewaka (1981). Plate tectonic evolution of Ethiopia and the origin of its mineral deposits: An overview. In: *Plate Tectonics and Metallogenesis: Some guidelines to Ethiopian Mineral Deposits*, Bulletin 2, pp. 115–119. Ethiopian Institute of Geological Surveys.

Divi, R., Zakir, F., and Al-Mishwat, A. (2001). Structure and Metallogenic framework of the Arabian Shield, the northern join between East and West Gondwana. *Gondwana Res.*, 4, 607–608.

Emily. J. Chin, Kei Shimizu, Grant M. Bybee, Monica E., and Erdman (2018). On the development of the calc-alkaline and tholeiitic magma series: A deep crustal cumulate perspective. Earth and planetary science letters, 482, 277-287.

Fritz, H., Abdelsalam, M., Ali, K.A., Bingen, B., Collins, A.S., Fowler, A.R., Ghebreab, W., Hauzenberger, C.A., Johnson, P.R., Kusky, T.M., Macey, P., Muhongo, S., Stern, R.J., and Viola (2013). Orogen styles in the East African Orogen: a review of the Neoproterozoic to Cambrian tectonic evolution. *J. Afr. Earth Sci.*

Ghebreab, W., Greiling, RO., and Solomon, S. (2009). Structural setting of Neoproterozoic mineralization, Asmara District, Eritrea. *J Afr Earth Sc*., 55, 219–235.

Gichile, S. (1992). Granulites in the Precambrian basement of southern Ethiopia: geochemistry, P-T conditions of metamorphism and tectonic setting. *Journal of African Earth Sciences*, 16, 251–263.

Golden Star Resources Limited (GSR) (1997). Ethiopia. DuI Gold Exploration Annual Report Year one May 31, 1996, and Year Two May 31, 1997

Grebennikov, A.V. (2014). A-type granites and related rocks: petrogenesis and classification, Russian Geology and Geophysics, 55, 1074-1086.

Guliev, G. (1982). Geochemical exploration in Asosa-Kurmuk-Gizen area of western Wellega between 1980 and 1982. U.N.D.P Project Ethio/80/016, Note No. 170

Holmes, A. (1951). The sequence of Pre-Cambrian orogenic belts in south and central Africa. 18th International Geological Congress, Great Britain. 1948. Part XIV, pp. 254–269.

Hugh, R. (1993). *Using geochemical data*: *Evaluation, Presentation, and Interpretation*. Pearson Education limited, England.

Irvine, G. J., and Baragar, W. R. (1971). A guide to the chemical classification of common volcanic rocks. *Canadian Journal of Earth Sciences*, 8, 523-548.

Johnson, P., Andresen, A., Collins, A.S., Fowler, A., Fritz, H., Ghebreab, W., Kusky, T., and Stern, R. (2011). Late Cryogenian–Ediacaran history of the Arabian-Nubian Shield: a review of depositional, plutonic, structural, and tectonic events in the closing stages of the northern East African Orogen. *J. Afr. Earth Sci*., 61, 167-232.

Johnson, T., Ayalew, T., Mogessie, A., Kruger, F., and Poujol, M. (2004). Constraints on the tectonometamorphic evolution of the Western Ethiopian Shield. Precambr Res 133, 305–327.

Johnson, T.E., Teklewold Ayalew, Abera Mogessie, Johan, F.K. and Poujol, M. (2004). Constraints of the tectononometamorphic evolution of the western Ethiopian shield. Precambrian research, 133, 305-327.

Jule, B**.** (2021). AFM diagram of igneous petrology. Available at: https://observablehq.com/@julesblm/afm-diagram-of-igneous-petrology

Kazmin, V. (1969). Geology of Tullu Kapi-Dalatti area. Unpublished Report, United-Nations

Kazmin, V. (1975). The Precambrian of Ethiopia and some aspects of the geology of the Mozambique Belt.- Bull. Geophys. Obs. Addis Ababa, 15, 27-18.

Kazmin, V., Shiferaw Alemu, and Balcha Tilahun (1978). The Ethiopian basement stratigraphy and possible manner of evolution. *Geol. Rundshau*, 67:531–546

Kebede, T., Koeberl, C., and Koller, F. (1999). Geology, geochemistry and petrogenesis of intrusive rocks of the Wallagga area, Western Ethiopia. *J Afr Earth Sci*., 29, 715–734

Kenea, D. (2017). Petrography And Deformation History Of Bila (Kidano King) Area Western Ethiopia. Unpublished MSc thesis, Addis Ababa University.

Kenea, D., Alemayehu, D., and Oljira, T. (2021) Geology and Structural Evolution of Neoproterozoic Rocks of Guliso Area, Wollega Western Ethiopia. *J Geol Geophys*, 10, 998.

Kennedy, WQ. (1964). the structural differentiation of Africa in the Pan-African ± 500 m.y. tectonic episode, 8th annual report on scientific results. University of Leeds, Leeds, p 50

Key, RM., Charlsey, TJ., Hackman, BD., Wilkinson, AF., and Rundle, CC. (1989). Superimposed Upper Proterzoic collision controlled orogenesis in the Mozambique orogenic belt of Kenya. Precambrian research, 44, 197–225

Kro¨ner, A. (1984). Late Precambrian plate tectonics and orogeny: a need to redefine the term Pan-African. In: Klerkx J, Michot J (eds) African geology. Musee Royal L'Afrique Centrale, Tervuren, pp 23–28

Kroner, A., Windley, B.F., Jaeckel, P., Brewer, T.S., and Razakamanana, € T. (1999). New zircon ages and regional significance for the evolution of the Pan-African orogen in Madagascar. *Journal Geological Society of London*, 156, 1125–1135.

Le Bas, M.J., Le Maitre R.W., Streckeisen, A., and Zanettina, B. (1986). A Chemical Classification of Volcanic RocksBased on the Total Alkali-Silica Diagram (on behalf of the IUGS Subcommission on the Systematics of Igneous Rocks). J. petrol., 27(83), 745-750.

Lulu Tsige (2008). Geology of Bure map sheet NC-37/5. Ethiopian Institute of Geological Survey.No.18.

McWilliams, M.O. (1981). Palaeomagnetism and Precambrian tectonic evolution of Gondwana. In: Kroner, A. (Ed.), Developments in € Precambrian Geology: Precambrian Plate Tectonics. Elselvier, Amsterdam, pp. 649–687.

Mengesha Tefera (1991). Geology of the kurmuk and assosa area memoir 7. Draft report, institute of geological survey of Ethiopia, Addis Ababa.

Mengesha Tefera and Seife Michael Berhe (1987). Geology of Sheet NC, 36-16,(Gore Sheet).

Mengesha Tefera, Tadiwos Chernet and Worklneh Haro (1996). Explanation of the Geological Map of Ethiopia. Ethiopian Institute of Geological Surveys, 2nd edition.

Mersha, J., Dawit, B., Anteneh, M., Bekana, M., Abayneh, T., Kassahun, Z., Abnet, Z. (1995). Final report of Dul Gold exploration Project. Dul Primary Gold Exploration and Development Project (DPGEDP), EIGS.

Middlemost, E.A.K. (1989). Iron oxidation ratios, norms and the classification of volcanic rocks. Chemical Geology 77, 19-26.

Moore, J.M., Morgan, J., Mengesha Tefera and Mengistu Teklay (1987). Geology of the Gore-Gambela Geotraverse, western Ethiopia. In: Current Research in African Earth Science, pp.109-112.A.A Balkema, Rotterdam

Muhongo, S., Kroner, A., Wallbrecher, E., and Sommer, H. (2001). Cross-section through the Mozambique Belt of East Africa and implications for Gondwana assembly. Gondwana Res. 4 (4), 709–710.

Mullen, E. (1983). Mno/Tio2/P2O5 Minor Element Discriminant for Basaltic Rocks Of Oceanic Environment and Implication for Petrogenesis. *Earth planet sci.lett,* 62,53-62

Natnael wondera (2018). petrogenesis of granitoid rocks of Assosa area, western Ethiopia. Unpublished MSc thesis, Addis Ababa University.

Nazemi, Ebrahim., Fatemeh, Ghotb, Tahriri, and Mostafa, B. (2015). Petrology and Geochemistry of Chaleh Kaftar Granites, Northeast of Torud. Article.10, 705-712.

Negussie, K. (1988). Preliminary draft report of Kurmuk Integrated Mineral exploration project. EIGS

Pinna, P., Jourdge, G., Calvez, JY., Morez, JP., and Margues, JM. (1993). The Mozambique Belt in northern Mozambique: Neoproterozoic (1100–850 Ma) crustal growth and tectogenesis and superimposed Pan-African (800–550 Ma) tectonism. Precambr Res 62, 1–59

Price, W.J. (1972). Analytical atomic absorption spectrometry. Heyden, London.

Richard, A., Batchelor and Peter Bowden (1983). Petrogenetic Interpretation of Granitoid Rock.

Roland, AI., and Joseph, AA. (2020). Petrography And Geochemistry Of Granitoid Rocks Around Fiditi, Southwestern Nigeria: Implications For Their Petrogenesis And Tectonic Setting. *Int.J. of Innovative Research and Advanced Studies (IJIRAS)*, 7(4), 89-100

Selamawit Abdissa (2018). Petrography and deformation history of basement rocks from Abay (Blue Nile) river around Agemsa town, western Ethiopia. Unpublished MSc thesis, Addis Ababa university.

Senbeto Chewaka (1980). Notes on the geology of part of Gimbi Sheet (NC36-12).Unpublished Report, Ethiopian Institute of Geological Surveys, 18pp.

Series Using Multicationic Parameters. *Chemical Geology*, 48, 43--55

Seyid, G. (2002) Geology of the Abu Ramla area. Geol Surv Ethiopia, Memoir 17:133S

Shackleton, R.M. (1986). Precambrian collision tectonics in Africa. In: Collision Tectonics. Geological Society. Special Publication, Vol. 19,pp. 329–352, (Coward, M.P. and Ries, A.C., eds). London.

Shackleton, R.M., (1996). The final collision zone between East and West Gondwana: where is it? *Journal of African Earth Sciences*, 23, 271–287.

Shelby Bowdena, Nahid, D., Gania , Tadesse Alemu , Paul O'Sullivan , Bekele Abebe, and Kibre Tadesse (2020). Evolution of the Western Ethiopian Shield revealed through U-

Pb geochronology, petrogenesis, and geochemistry of syn- and post-tectonic intrusive rocks; Precambrian Research 338 (2020) 105588. https://doi.org/10.1016/j.precamres.2019.105588

Soukhoroukov (1980). Geology and geochemical prospecting for gold and tungsten in Kurmuk areas, Western Wellega. Ethiopian Institute of Geological Surveys Technical Report

Stern, R.J. (1994). Arc assembly and continental collision in the Neoproterozoic East African orogen. Ann. Rev. Earth Planet. Sci., 22, 319–351.

Stern, R.J. (1994). Arc assembly and continental collision in the Neoproterozoic East African orogen. Ann. Rev. Earth Planet. Sci., 22, 319±351.

stern, R.J., Kamal, A., Mohamed, A., Abdelsalam, G., Simon, A., and Wilde, Qin Zhou. (2012). U-Pb Zircon geochronology of the eastern part of the Southern Ethiopian Shield. Precambrian research, 159-16.

Stern, RJ. (1994). Arc assembly and continent collision in the Neoproterozoic East African Orogen: implication for the consolidation of Gondwanaland. Annal Rev Earth Planet Sci, 23, 289–310

Stern, RJ. (2002). Crustal evolution in the East African Orogen: a neodymium isotopic perspective. *J Afr Earth Sc*, 34, 109–117

Stern, RJ., Ali, KA., Abdelsalam, MG., Wilde, SA., and Zhou, Q. (2010b) U–Pb Zircon geochronology of the eastern part of the Southern Ethiopian Shield. Precambr Res, 206–207. & 159–167.

Stern, RJ., Ali, KA., Liégeois, J-P., Johnson, P., Wiescek, F., and Kattan, F. (2010a). Distribution and significance of pre-Neoproterozoic zircons in juvenile Neoproterozoic igneous rocks of the Arabian-Nubian Shield. *Am J Sci*, 310,791–811.

Stern, RJ., and Dawoud, AS. (1991). Late precambrian (740 Ma) charnockite, enderbite and granite from Jebel Moya: a link between the Mozambique Belt and the Arabian-Nubian Shield? *J Geol*, 99, 648–659.

Stern, RJ.,and Kröner, A. (1993). Late Precambrian evolution in NE Sudan: isotopic and geochronological constraints. *J Geol*, 101, 555–574.

Sylvester, P. J.(1989). Post - collisional alkaline granites. *Journal of Geology*, 97, 261-280.

Tadesse Alemu and Tsegaye Abebe (2007). Geology and Tectonic Evolution of the Pan-African Tulu-Dimtu Belt, Western Ethiopia. *Online Journal of Earth Sc.*, 1, 24–42.

Tadesse Yihunie and Fekadu Hailu (2007). Possible eastward tectonic transport and northward gravitational tectonic collapse in the Arabian-Nubian shield of western Ethiopia. *Journal of Africa Earth Sciences*, 49, 1-11.

Tadesse, G., and Tesfeye, M. (1999). The geology of the Tosho Sheet (NC36-11). Unpublished Technical Report, Regional Geology and Geochemistry Department, Ethiopian Institute of Geological Surveys, 42 pp.

Tadesse, T. (1996). Geology of the Axum area. Geol Surv Ethiopia, Memoir 9, 192.

Tefera, M. (1991) Geology of the Kurmuk and Asosa areas. Ethiopian Institute of Geological Surveys, draft report, p 109

Teklay, M. (1986). Petrology and geochemistry of supracrustal and intrusive rocks from the Birbir Domain of the Gore-Gambella Geotraverse. MSc Thesis, Addis Ababa University.

Teklay, M., Kroner, A., Mezger, K., and Oberhansli, R. (1998). Geochemistry, Pb-Pb single zircon ages and Nd-Sr isotope composition of Precambrian rocks from southern and eastern Ethiopia: implications for crustal evolution in East Africa. *J. Afr. Earth Sc.*, *26*(2), 207–227.

Teklay, M., Kroner, A., Oberh, €., and €ansli, R. (1993). Reconnaisance Pb–Pb zircon ages from Precambrian rocks in eastern and southern Ethiopia and an attempt to define crustal provinces. In: Thorweihe, U., Schandelmeier, H.J. (Eds.), Geoscientific Research in Northeast Africa. Balkema, Rotterdam, pp. 133–138.

Teklewold Ayalew (1997). Metamorphic and structural evolution of the Gore-Gambella area, Western Ethiopia. SINET: *Ethiop. J. Sci.*, 20(2), 235–259.

Teklewold Ayalew and Johnson, T.E. (2002). The Geotectonic Evolution of the Western Ethiopian Shield. SINET, 25, 227–252.

Teklewold Ayalew and Moore, J.M. (1989). The Gore-Gambella Geotraverse, Western Ethiopia. Open File Report – IDRC; 153 pp.

Teklewold Ayalew and Peccerillo, A. (1998). Petrology and geochemistry of the Gore-Gambella plutonic rocks: implications for magma genesis and the tectonic setting of the pan-African Orogenic Belt of western Ethiopian. *Journal of African Earth Sciences*, 27, 397-416.

Teklewold Ayalew, Bell, K., Moore, J.M., and Parrish, R.R. (1990). U-Pb and Rb-Srgeochronology of the Western Ethiopian Shield. Geology Soc .Am .Bull, 102, 1309-1316.

Tesfaye Kebede and Koeberl, C. (2002). Petrogenesis of A-type granitoids from the Wallagga area, western Ethiopia: constraints from mineralogy, bulk-rock chemistry, Nd and Sr isotopic compositions. Precambrian Research, 121, 1–24.

Tesfaye Kebede and Koeberl, C. (2003). Petrogenesis of A-type granitoids from the Wallagga area, Western Ethiopia: constraints from mineralogy, bulk-rock chemistry, Nd and Sr isotopic composition. Precambrian Res. 121, 1–24.

Tesfaye Kebede, Kloetzli, U.S., and Koeberl, C. (2001). U/Pb and Pb/Pb zircon ages from granitoid rocks of Wallagga area: constraints on magmatic and tectonic evolution of Precambrian rocks of western Ethiopia.Mineralogy and petrology, 71, 251-271.

Tesfaye Kebede, Koeberl, C., and Koller, F. (1999). Geology, geochemistry and petrogenesis of the Neoproterozoic orogenic belt of Tuludimtu, Western Ethiopia. *Journal of African Earth Sciences*, 36, 329–343.

Tsige, L. (2006). Metamorphism and gold mineralization of the Kenticha-Katawicha area: Adola belt, southern Ethiopia. *J. Afr. Earth Sc*., 45, 16–32.

Tsige, L. (2008). Geology of the Bure area. Geological Survey of Ethiopia, Memoir 18:

Warden, AJ., Kasmin, V., Kiesel, W., and Pohl, W. (1982). Some geochemical data of mafic–ultramafic complex at Tulu Dimtu, Ethiopia and their genetic significance. *Sitzungsberichte Osterreichische Akad Wissenschaft Math Naturwissenschaft*, 191, 111–131.

Woldemichael, B.W., Kimura, J.-I., Dunkley, D.J., Tani, K., and Ohira, H. (2010). SHRIMP U–Pb zircon geochronology and Sr–Nd isotopic systematic of the Neoproterozoic Ghimbi Nedjo mafic to intermediate intrusions of western Ethiopia: a record of passive margin magmatism at 855 Ma? *Int. J. Earth Sci.*, 99, 1773–1790.

Wollie, S., Negussie, K., Abnet, Z., Tesfaye, T., Tibebu, T., Alemayehu, M., Alelign, M., Abera, F., Tesfu, T., Getahun, B., Kone, F., and John, Z. (1990). Geology and mineralization of Dul and Azale-Akendeyu. Kurmuk Integrated Mineral

Exploration Project, Ethiopian Institute of Geological Surveys technical report 821-351-42:62.

Yibas, B., Reimold, W., Armstrong, R., Koeberl C., Anhaeusser, C., and Phillips, D. (2002). The tectonostratigraphy, granitoid geochronology and geological evolution of the Precambrian of southern Ethiopia. *J Afr Earth Sc*, 34, 57–84.

Yihunie, T. (2003). Chemical Th-U-total Pb isochron ages of zircon and monazite from granitic rocks of the Negele area, southern Ethiopia. J. *Earth Planetary Sc.*, 50, 1–12.

Zakaria Hamimi, Abdel-Rahman Fowler, Jean-Paul Liégeois, Alan Collins, Mohamed G. Abdelsalam, and Mohamed Abd EI-Wahed (2021). *The Geology of the Arabian-Nubian Shield*. Roland Oberhänsli, Francois Roure, and Dirk Frei.

Zuber, A. (1986). Preliminary draft geological map (1:250,000) of the Kurmuk-Assosa area.

Appendixes

Appendix-1 Field description of the representative rock samples

Sample name	Location		descriptions
	Northings	Easting	
D1S-1	0665612	1159465	Greenish black in color, fine to medium-grained and massive.
D2S-1	0665538	1159198	Hard, fine-grained, greenish black color, and reddish weathered-color
D2S-2	0665798	1158647	Quartz precipitates from the openings. The openings filled with reddish materials. The rock is amygdaloidal basalt
D2S-4	0667518	1156978	Fine-grained, black colored rock. It is highly weathered
D2S-5	0667518	1156978	Very fine-grained light colored rock
D3S-1	0669826	1154436	Black colored basaltic rock and slightly weathered
D3S-2	0670330	1155699	Fine-grained light colored rock
D3S6	0672035	1155958	Fine to medium grained rock. It slightly light colored.

D3S-7	0672119	1155214	Fine to medium-grained meta-granitic rock. White colored quartz and feldspar mineral is seen
D4S-1	0677885	1135340	Medium to coarse-grained rock with the dominant of biotite and quartz. The biotite minerals are seen in dark color while the felsic minerals are showing light colors
D4S-1G	0677885	1135340	Highly deformed at the contact. Ranges from fine to medium-grained

Appendix-2 modal percentage of the minerals seen under petrographic microscope in the representative samples

Sample name	quartz	kfs	plag	olv	bt	hbl	opq	pyx	others
D1S-1	-	-	55%	40%	-	3%	1%	1%	
D3S-7	45	45	5		5				
D4S-1	20	30	10%	10%	25	5	-	10	-
D4S-1G	35%0%	60%	-	-	5	-	-	-	-

Appendix-3: definition of terms

Amalgamation: A phrase applied in geoscience to refer to the procedure through which several distinct deposits of minerals combine to form one deposit. The concept of "amalgama," which means "a combination of different metals," is taken from Latin, giving rise to the name. If accumulations of minerals are found near one another and are exposed to tectonic processes allowing to their mix, amalgamation may take place.

Concordant: The type of igneous parallel intrusion with the stratification of the underlying rock is 'referred' to as being concordant by the geological word. The word's root, "concordare," is a Latin verb that means "to agree."

Holocrystalline: A word utilized in geoscience to designate rocks made completely of crystals. The name consists of two Greek words combined, "holos," which means "complete," and "krustallos," which means "crystal." Magma or lava that has been slowly cooled typically crystallizes into holocrystalline rocks.

Juvenile: a word employed in geoscience for referring to rocks which have not yet undergone the stages of crystallization or differentiation. These rocks are generated from magma. The expression "juvenis" is a derivative of Latin and means "young" in English. Younger rocks are often discovered in volcanic areas and are distinguished by a substantial amount of flammable substances like water and carbon dioxide.

Leucocreatic: a phrase applied in geoscience to refer to rocks which are bright in color because they contain minerals with a similar color, including feldspar and quartz. The name originates from the Greek terms "kratos," which means power, and "leukos," which means white..

Migmatite: An igneous rock of the variety distinguished by the size that constitutes its crystals. Pegmatites are frequently discovered among various other types of rocks like granite and gneiss.

Ophiolite: a phrase used in geoscience to denote a group of rocks accessible on lands that were created from the lithosphere of the ocean. The word consists of two Greek words combined, "ophis," which means "snake," and "lithos," which means "stone." Ophiolites are defined by their distinctive arrangement of rocks, including peridotite, gabbro, sheeted dikes, with pillow lavas. They are seemed to be prevalent in mountainous systems.

Pilotaxitic: The expression "pilotaxitic" originated from the Greek words "pilotos" (which means "guide") and "axis" (which means "axis") and has applications in ‘earth sciences’ to refer to an appearance of igneous material which is defined by an abundance of lengthened crystals which are directed in a similar orientation.

Psammitic: a phrase used in geoscience to characterize rocks that have sand-sized particles as their main constituents. The expression "psammos" is a Greek word that means "sand" and is where the phrase originates.

Tibetan-type collision/volcanism: The eruptions of volcanoes that took place throughout the Tibetan Plateau territory is referred to as "Tibetan-type volcanism." Immense in size and located in Central Asia, the ‘Tibetan Plateau’ has been known as being the "Roof of the Globe" because of its altitude. Numerous living and dead volcanoes may be found on the plateau, and is ‘thought’ to have ‘resulted’ from the clash of Indian and the Eurasian continental plates.

Truncated: a phrase that refers to the point at which a rock structure or layer ends up along a surface that is uneven. The expression "truncatus" means "cut off" in Latin, from which the phrase is taken.

Verging: is an expression applied to geoscience to define how rock strata or faults are oriented. Once layers of rock or faults are described as "verging," it signifies that they are sloping slightly in the direction of one another. The phrase is frequently used in reference to fold and 'thrust belts', which are geographical areas whereby rocks have undergone tectonic deformation.